CHAPTER 3: *IN SITU* LASER-ABLATION-ICP-MS CHEMICAL ANALYSIS OF MELT INCLUSIONS AND PROSPECTS FOR CONSTRAINING SUBDUCTION ZONE MAGMATISM

Thomas Pettke
University of Bern, Institute of Geological Sciences,
Baltzerstrasse 1+3,
CH–3012 Bern, Switzerland
pettke@geo.unibe.ch

INTRODUCTION

Melt inclusions (MI) may provide direct samples of parental liquids during growth of their host crystals (*e.g.,* Anderson 1974, Clocchiatti 1975, Watson 1976, Roedder 1979, Sobolev 1996, Lowenstern 1995, Frezzotti 2001, Schiano 2003). They may form in virtually all types of phenocrysts; hence MI compositions monitor the chemical changes of the residual liquid during magma evolution. Thanks to petrographic and petrologic control of the host mineral crystallization and MI entrapment sequence, such data provide powerful constraints on source magma characteristics and on (deep) processes such as fractional crystallization, assimilation, magma mixing and volatile saturation. Such detailed resolution of chemical signatures using MI holds potential for resolving the chemical evolution of magmatic systems in great detail. This, in turn, provides an excellent tool for elucidating igneous processes at various scales and stages in different geotectonic settings.

Melt inclusions are commonly only up to a few tens of micrometres in diameter; hence, an *in situ* microbeam technique is required to analyze their chemical composition (for reviews see *e.g.,* Roedder 1984, Ihinger *et al.* 1994, Lowenstern 1995). Melt inclusions may undergo several transformations after entrapment such as crystallization, fluid exsolution or diffusive equilibration with host minerals and external magma, collectively called post-entrapment modifications (*e.g.,* Danyushevsky *et al.* 2000, 2002, Tait 1992, Watson 1976, Sobolev & Chaussidon 1996, Gaetani & Watson 2000, Qin *et al.* 1992, Kress & Ghiorso 2004). Therefore, it is not trivial to backtrack to the correct chemical composition of the original liquid. Limited understanding of these complications is probably the principal reason for the limited acceptance of quantitative MI data in igneous petrology.

Traditionally, electron probe microanalysis (EPMA) and secondary ion mass spectrometry (SIMS) have been utilized to analyze a fraction of the total MI exposed at the sample surface. Pioneering work using laser ablation–inductively coupled plasma–mass spectrometry (LA–ICP–MS) followed the same approach, drilling pure MI material out of the sample (Taylor *et al.* 1997). Most LA–ICP–MS MI applications since have provided an alternative to SIMS analysis, notably for middle to heavy trace elements (*e.g.,* Taylor *et al.* 1997, Kamenetsky *et al.* 1999, de Hoog *et al.* 2001, Kamenetsky *et al.* 2002). Obviously, polyphase MI have to be homogenized in the lab to produce a homogeneous single phase (glass) followed by exposure to the sample surface for analysis. Having obtained a glass, the analyst can test for homogeneity by measuring multiple spots on exposed large MI. However, the mere presence of a homogeneous glass in the MI after homogenization does not guarantee that this glass is chemically representative of the originally trapped melt. An incorrect amount of host mineral may have been remelted into the MI, or the melting conditions of the MI were modified in response to volatile loss, *e.g.,* H_2 or H_2O. As a consequence, a large variety of crystallized MI exists from various geotectonic settings, notably from volatile-rich plutonic rocks, that cannot be homogenized to a glass by heating them up to independently estimated entrapment temperatures. If heating to considerably higher temperatures is required to remelt a crystallized MI, this suggests volatile loss, resulting in a glass composition that will not be identical to that of the melt at the time of entrapment. In light of the above concerns, some researchers have tried to identify and investigate samples with minimal extent of post-entrapment modifications in subduction zone settings, for example, from tephra, small diameter lapilli or tuff/ash. Shortcomings of possible sampling bias towards naturally glassy MI or MI that could be homogenized in the lab at entrapment

---

Mineralogical Association of Canada Short Course 36, Montreal, Quebec, p. 51-80.

temperatures is thus a serious concern notable for investigations of hydrous plutonic systems.

A unique feature of LA–ICP–MS is the possibility to analyze *heterogeneous MI* as entire inclusions and to reconstitute their bulk chemical composition. Consequently, all types of MI can now be analyzed for major to trace element compositions, considerably expanding the MI applications in igneous petrology. This paper focuses on the technique of bulk chemical MI analysis by LA–ICP–MS as an alternative approach in MI research in an attempt to illustrate its potential for investigations related to hydrous plutonic systems where crystallized MI are ubiquitous. This development builds on pioneering work devoted to the chemical analysis of entire fluid inclusions by LA–ICP–MS (*e.g.,* Ramsey *et al*. 1992, Günther *et al.* 1998). The analysis of entire MI drilled out of the host crystal thereby represents the most general case of bulk inclusion analysis.

This contribution presents first a discussion of fundamental parameters in LA–ICP–MS. A strategy for the optimization of LA–ICP–MS analytical conditions for geological materials is then presented, with special attention to the analysis of entire MI in minerals. Analysis and data quantification strategies of LA–ICP–MS bulk MI analysis are then outlined and compared primarily to those of SIMS and EPMA, followed by a discussion of the strengths and limitations of these techniques. A detailed discussion of SIMS applications is provided by Layne (2006); an excellent book on principles of EPMA published by Goldstein *et al*. (1992). This chapter then concludes with an introduction to the small, nascent literature bearing on bulk MI analysis from plutonic rocks in subduction zones and on experimental work constraining the chemical composition of aqueous fluids and hydrous melts and supercritical fluids coexisting with eclogite. These examples shall elucidate the prospects of the novel approach of LA–ICP–MS analysis of heterogeneous samples such as crystallized MI to constraining subduction zone magmatism.

Background

Before discussing the various analytical approaches in more detail, I consider it necessary to briefly review some inclusion terminology, MI entrapment conditions and the various possibilities of reversible or irreversible post-entrapment modifications (as far as is currently recognized). These issues are relevant for MI research in general, yet their significance may vary considerably with analytical techniques employed. For a comprehensive treatment of principles of MI research the reader is referred to the contribution of Bodnar & Student (2006).

Careful petrographic characterization of MI types in phenocrysts and xenocrysts in a given rock sample is a prerequisite for later interpretation of analytical data. The aim of this characterization is to establish the entrapment sequence of MI present in the sample, providing a window on the chemical evolution of the magmatic system. Fig. 3-1 shows a sketch illustrating some petrographic key observations and illustrates the basic concept of MI assemblages.

When phenocrysts grow, they commonly trap the liquid from which they crystallize as inclusions. Several coevally entrapped inclusions are termed an inclusion assemblage (Fig. 3-1). We distinguish homogeneous and heterogeneous assemblages. Homogeneous assemblages (Fig. 3-1) contain inclusions of *originally identical* chemical composition (excluding possible boundary layer effects). Each inclusion of such an assemblage thus represents an isolated sample of a chemically uniform melt at the time of entrapment. Heterogeneous assemblages are coevally entrapped inclusions of variable chemical composition, for example coexisting melts (such as silicate and sulfide melts) or coexisting silicate melt and aqueous fluids (Fig. 3-2C). Such assemblages contain inclusions of both immiscible phases, possibly together with inclusions representing mixtures between the two end members.

An assemblage of primary MI represents inclusions coevally trapped while the host crystal grew (Fig. 3-1). Hence, such MI assemblages commonly line growth zones in phenocrysts (Figs. 3-1, 2A). Assemblages of secondary MI represent inclusions that formed after the host crystals grew (Fig. 3-1). Hence, the chemical compositions of the host mineral and the secondary inclusions are most likely not related to each other. Typically, assemblages of secondary MI fill former cracks oblique to growth zoning in host minerals, and such cracks commonly cut through grain boundaries. Secondary MI assemblages may be common in xenocrystic minerals or grain aggregates (Fig. 3-1). Consequently, the correct identification of secondary inclusions is crucial for MI studies. It is important to appreciate that inclusions in proper assemblages may appear petrographically variable

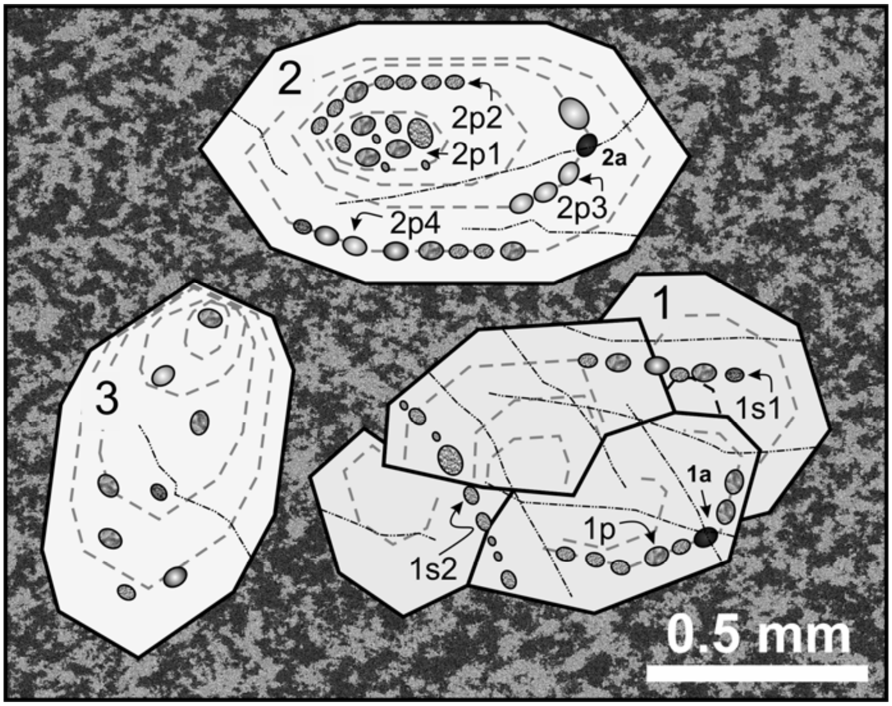

FIG. 3-1: Sketch of a rock thick section showing different petrographic types of melt inclusions (MI). One xenocrystic aggregate consisting of 4 crystals (number 1) and two phenocrysts (crystal 2 and 3) are set in a fine-grained groundmass. Each crystal shows former growth zones outlined in dashed, grey lines. Cracks in crystals are shown by thin dashed, black lines. Crystal 2 hosts primary MI assemblages (labeled 2p1, 2p2, 2p3, 2p4). Individual MI are either arranged along planes (as can be recognized by varying focal depth during thick section microscopic observation) parallel to the crystal surfaces or cluster in a part of the crystal, here shown in the core. One assemblage in aggregate 1, labeled 1p, is also primary, while the other two MI assemblages, labeled 1s1 and 1s2, are secondary. The latter cut across growth zoning of individual crystals, across grain boundaries within the xenocrystic aggregate, and they sometimes reach the crystal surfaces (assemblage 1s2). MI in phenocryst 3 are characterized by a geometrically random occurrence; hence, they cannot be grouped into assemblages. MI labeled 1a in xenocryst aggregate 1, and 2a in phenocryst 2, are cut by a crack. These MI should be avoided because of the possibility of alteration through fluids that circulated through the crack (indicated by the dark appearance of the respective MI). Petrographic interpretation of this sample is that the oldest MI are represented in assemblage 1p, recording a magmatic event prior to formation of this rock. Assemblages 2p1, 2p2, 2p3 and 2p4 were successively trapped while phenocryst 2 grew; hence, they record the melt evolution while this rock crystallized. The MI in phenocryst 3 are randomly distributed throughout the crystal. They can only be arranged into an entrapment sequence when growth zoning of the host crystal is independently visible. This is a rare case. Commonly, such MI cannot be reliably used to establish the chemical evolution of the melt while the crystal grew and, therefore, such MI should be avoided whenever possible. Note in the example of phenocryst 3 that the MI closest to the rim of the phenocryst is actually the oldest one in this phenocryst. Secondary inclusion assemblages 1s1 and 1s2 are not useful either because they may have trapped a melt prior to inclusion of the xenocrystic aggregate 1 in this magma, or they may contain melt from this magma trapped shortly before its solidification.

(Figs. 3-1, 2A) due to different extents of post-entrapment modifications explained in detail below.

Melt inclusion populations commonly encompass all inclusions trapped, for example, in one phenocryst type. In Figure 3-1, the MI hosted by phenocrysts 2 and 3 could be unified into a MI population. A MI population, therefore, commonly contains several inclusion assemblages successively entrapped while the host phenocryst grew (obvious for phenocryst 2 but not for phenocryst 3) and the residual melt evolved. Hence, MI of a population are expected to be chemically variable and may thus not provide precise average chemical compositions of temporally well-resolved crystallization stages.

Melt inclusions are useful probes of the melt present in magmatic evolution only when they represent equilibrated melt droplets. Two principal processes of MI entrapment exist, illustrated based on MI formation in olivine, (a) diffusion-controlled and (b) equilibrium entrapment (see Faure &

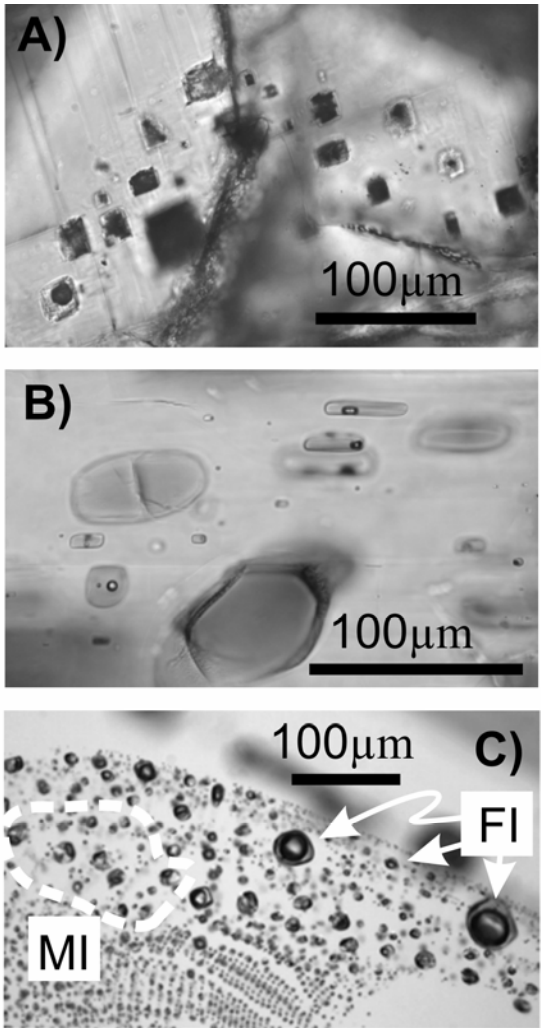

FIG. 3-2: Photomicrographs of various inclusion types. Image (A) shows a variably crystallized melt inclusion (MI) assemblage in plagioclase from an andesite, lining a former growth zone. Note the variable appearance of inclusions all with negative crystal shapes, from glassy with bubble (bottom left) to completely devitrified (black, without visible bubble). (B) Glassy MI in plagioclase from a dredged MORB sample showing variably sized shrinkage bubbles. (C) Heterogeneous assemblage of co-existing silicate melt (MI cluster outlined by dashed white line) and vapor-like fluid inclusions (FI identified by white arrows) in quartz (from Audétat and Pettke, 2003). Note the presence of inclusions of various mixing proportions between the two end member phases.

Schiano, 2005, for a detailed discussion and excellent MI images). Diffusion-controlled MI formation represents disequilibrium entrapment; the material enclosed in the MI corresponds to the boundary layer forming around dendritic or skeletal crystals. Equilibration of this boundary layer with the rest of the melt through diffusion is not possible because diffusion is too slow. Therefore, the boundary layer will be relatively depleted with elements compatible in the host, and enriched in the incompatible ones; diffusive supply of components limits the growth rate of the crystal. Resulting MI are chemically heterogeneous and may display chemical trends as a function of MI size which may be revealed when working with MI assemblages (the "boundary layer effect" commonly referred to in the literature). During equilibrium entrapment, interface attachment processes control MI formation (*i.e.*, host mineral growth rate controlled) and the host forms polyhedral crystals. Resulting MI are chemically representative of the residual melt, irrespective of their size. Careful petrography is thus required to study the morphology of host phenocrysts in order to avoid MI assemblages that may suffer from boundary layer effects. Another point of concern is the possibility of accidentally trapped minerals in MI, having once served as a nucleus for MI formation. Such MI, too, can be identified when working with MI assemblages. Finally, MI in primitive (*i.e.*, Fo-rich) olivine may not have sampled "geologically significant melt bodies" but rather the product of localized dissolution–reaction–mixing processes in mush zones of the magmatic plumbing system (*e.g.*, Danyushevsky *et al.* 2004).

The above statements emphasize the prerequisite of careful sample selection and petrographic inspection of MI for conducting a "meaningful MI study" including addressing issues of post-entrapment modifications (*e.g.*, Roedder 1979, 1984). Two types of post-entrapment modifications need clear distinction, those which can be reversed in the lab by bringing the inclusion back to entrapment conditions, and those which irreversibly modify inclusion compositions.

Every MI evolves after entrapment and may eventually nucleate a bubble inside the glass (Fig. 3-1). This bubble either forms in response to fluid exsolution from the trapped melt (for inclusions that trapped a melt near or at fluid saturation), or it may represent a shrinkage bubble resulting from post-entrapment crystallization of the host mineral onto the inclusion walls (for inclusions that trapped a strongly fluid-undersaturated melt). Such bubbles form before the MI reaches the temperature of the glass transition; hence, they provide indications of significant high-temperature fluid exsolution or sidewall crystallization. The extent of this crystallization obviously varies with the extent of chemical difference between the MI and host mineral composition (the more similar they are, the larger the mass fraction of post-entrapment host crystallization may be) and with the post-entrapment history of the MI. Intuitively, these post-entrapment effects are minimized for quenched extrusive rocks as illustrated by the large amount of research dedicated to MI studies on volcanic ejecta from various geotectonic settings. Such MI can commonly be reverted to entrapment composition by reheating to entrapment temperature in the lab (*e.g.,* Anderson 1974). Yet, much microbeam analytical work has been done on glassy untreated MI, thereby measuring a composition that may be more evolved than that present at the time of entrapment (*e.g.,* Danyushevsky *et al.* 2002, Pettke *et al.* 2004). If such precise microbeam measurements are directly used for petrogenetic modelling, results may be seriously misleading. Such data require correction by modelling the reverse of host mineral crystallization onto the inclusion walls (*e.g.,* Danyushevsky *et al.* 2000, de Hoog *et al.* 2001¸ Kress & Ghiorso 2004, Pettke *et al.* 2004) to obtain the correct chemical composition at entrapment. For the case of fluid bubble exsolution prior to solidification of the MI, volatile elements and some metals (*e.g.,* Cu, Zn, Pb) will be strongly enriched in the bubble, and the analysis of the exposed glass of unheated MI will seriously underestimate the contents of such elements in the melt at the time of entrapment.

Irreversible post-entrapment modifications are readily indicated if homogeneously trapped MI do not homogenize to a glass at entrapment conditions (note that designing a MI reheating experiment requires optimization of the heating rate: as fast as possible to minimize H_2 diffusion out of MI but slow enough to satisfy kinetic limitations of melting; Danyushevsky *et al.* 2002). These modifications include all cases where mass transfer occurred through the MI–host mineral interface. The extent of such modifications ranges considerably, from diffusive loss of volatiles (most importantly H^+ or H_2O), to diffusive re-equilibration with the host mineral (*e.g.,* Fe and Mg in mafic minerals) or even the external magma at elevated temperatures (either during natural slow cooling and/or during reheating in the lab), to chemical exchange with extraneous components introduced along cracks in the host (*e.g.,* Gaetani & Watson 2000, Danyushevsky *et al.* 2000, 2002, Qin *et al.* 1992, Tait 1992, Hauri *et al.* 2002, Luhr 2001, Metrich & Clocchiatti 1996, Sisson & Layne 1993, Cottrell *et al.* 2002). Model predictions by Gaetani & Watson (2000) suggested that diffusive equilibration may be a problem when strong chemical gradients are present between the MI and its surroundings. Some MI may even decrepitate, notably in host minerals other than quartz, or MI may suffer from decrepitation of fluid inclusions in the same mineral grain when reheated in the lab at atmospheric pressure conditions (*e.g.,* Roedder 1984, Tait 1992, Webster *et al.* 1997, Student & Bodnar 2004). Introduction of Cu and Ag into the MI from the crucible in which quartz phenocrysts were heated for 24h at 850°C has been demonstrated (Kamenetsky & Danyushevsky 2005) and illustrate that even the environment of lab treatment may adulterate the bulk MI composition.

It is important to appreciate that while the concentrations of some elements or species in the inclusions may have been modified irreversibly in nature or in the lab, others (*e.g.,* the large ion lithophile elements and the rare earth elements in MI hosted by plagioclase, olivine or orthopyroxene) may have remained largely unaffected (see *e.g.,* Schiano, 2003). There is a clear need to improve our understanding of the extent of diffusive equilibration in natural samples. Volume diffusion data only provide a conservative estimate of the problem, because imperfections providing fast diffusion tracks are likely to control the rate of diffusive exchange. The artistry in MI research is to determine which element concentrations of any given MI assemblage have remained unadulterated and thus can be used for petrogenetic modeling.

MICROBEAM INSTRUMENTATION

The following section will summarize key application characteristics of LA–ICP–MS and compare them with other techniques (*e.g.,* EPMA, SIMS, Fourier Transform Infrared Spectroscopy (FTIR) and RAMAN scattering) that are applicable to the analysis of MI. This discussion is preceded by a more fundamental consideration of key parameters and an optimization strategy for the accurate analysis of geological materials by LA–ICP–MS. The comprehensive description of these analytical techniques is beyond the scope of this paper, and the interested reader is referred to the literature cited below. Rather, a conceptual path is followed. We have geoscientific questions to be answered through the analysis of a series of MI. We try to appraise the type of data that can be obtained by using the various microbeam techniques, and we try to appreciate the significance of these data sets. It will be illustrated that LA–ICP–MS is the only method to date for the bulk chemical analysis of MI that cannot be homogenized reliably in the lab. Such MI may be dominant in some hydrous magma types; hence, LA–ICP–MS MI analysis has an enormous potential to constrain better subduction zone magmatism and plutonic activity in particular.

All analytical instruments share the common principle that a beam smaller than ca. 200 µm is focused on the sample and emits radiation or sample material to be measured by a detection device. An important consequence of this approach is that the response of any analytical setup is calibrated against standard materials of known composition and state (crystalline, amorphous). We distinguish two principal analytical setups. In setup one, the signal (ions or radiation) emitted from the analytical spot on the sample is directly measured (EPMA, SIMS, Raman, FTIR, or Laser-Induced Breakdown Spectroscopy (LIBS)). LIBS will not be considered further here because this technique is extremely matrix–dependent. In setup two, sample material is liberated and transported as an aerosol to a site where the signal (ions or radiation) is produced independently of the sample liberation process (LA–ICP–MS and LA–ICP–Optical Emission Spectroscopy (OES)). LA–ICP–OES will not be considered further in this contribution because limits of detection (LOD) are not competitive with LA–ICP–MS for the vast majority of elements (*e.g.,* Pettke *et al.* 2000). LA–ICP–MS has a key advantage, namely that it allows independent optimization of two fundamentally different processes, sample ablation and production of ions in the ICP for analysis. This can considerably reduce matrix effects on analyte signals, provided that other key LA–ICP–MS parameters are properly taken into account. Consequently, the need for strictly matrix-matched calibration, a prerequisite for SIMS analysis and recommended for EPMA, may be strongly relaxed for LA–ICP–MS analysis.

LA–ICP–MS analytical setup

All commercially available LA–ICP–MS setups consist of a pulsed monochromatic laser source, laser beam modulation optics, a modified petrographic microscope with TV screen observation and an ICP–MS instrument (Fig. 3-3). Various LA–ICP–MS systems have significantly different but interrelated key parameter specifications. The following paragraphs elaborate on laser beam properties and ICP–MS settings I consider particularly relevant for the analysis of geological samples in general and MI in particular. For a complete list of parameters the reader is referred to Günther & Hattendorf (2005). Note that most results in the literature were obtained by using a specific LA–ICP–MS instrumental setup, and the various setups used possess considerably different specifications. It is therefore delicate to generalize conclusions that were obtained by one given setup. This is also the reason why there are not many numbers provided in the following section. Rather, the reader should get confronted with some basic principles about LA–ICP–MS parameters and their mutual dependence.

Laser energy and its spatial energy profile (*i.e.,* energy distribution across the ablation pit) are of paramount importance. First, enough energy density on the sample surface is required to effect ablation. This energy density is also called irradiance (energy per area, W/cm^2) per pulse and relates to the laser fluence. The laser fluence is the total amount of energy per area (J/cm^2) per pulse reaching the target, which is proportional to the output energy of the laser system. For fixed laser output energy, the irradiance will increase with decreasing laser pulse duration.

Each material has a characteristic energy density below which ablation does not occur and the material may crack or splinter. For quartz, this ablation energy threshold corresponds to a narrow window in energy density that is variable between ~10 and 20 J/cm^2 (for 193 nm excimer laser light of ~20 ns pulse duration) for different quartz samples. For example, when the ablation energy threshold is 15 J/cm^2 for a given quartz sample, then no ablation occurs below ~13 J/cm^2 while perfect ablation is observed above ~17 J/cm^2. The ablation energy threshold is generally lower for mafic minerals. For a laser fluence above the ablation threshold and silicate or oxide matrices, typical ablation rates for 193 nm excimer laser light are 100–200 nm per pulse. Ablation rates for a given analytical setup increase linearly with increasing laser fluence for ns-pulsed UV laser light (*e.g.,* Horn *et al.* 2001).

It follows from the above observations that identical ablation conditions throughout the entire pit, between successive laser shots and for variable pit sizes facilitate controlled ablation. For non-homogenized energy laser beams, some parts of the ablation pit (*e.g.,* rim domains) may not reach controlled ablation conditions because of

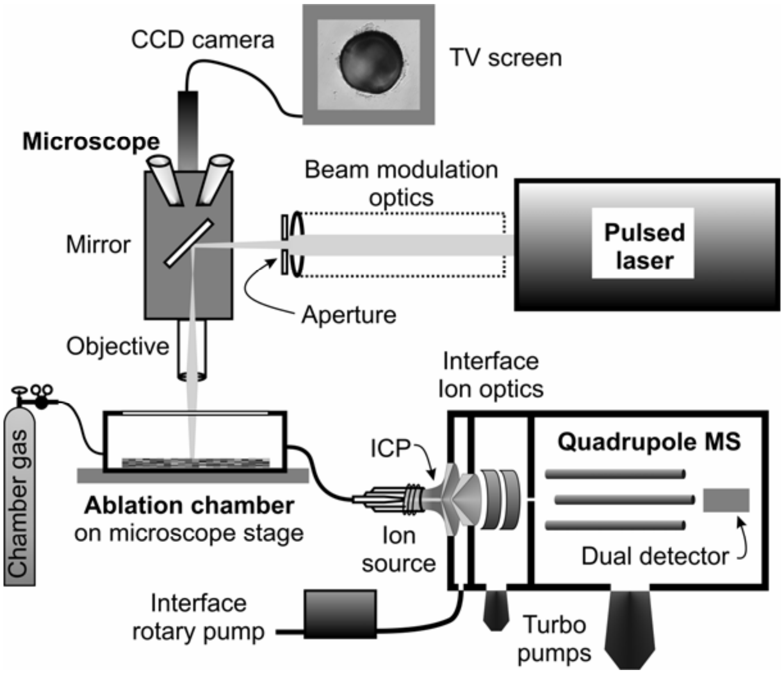

FIG. 3-3: Sketch of a laser – ablation inductively – coupled – plasma mass – spectrometry (LA–ICP–MS) setup, consisting of a laser source, beam modulation optics, a microscope equipped with camera and TV screen (showing a 40µm pit in quartz), and a commercial quadrupole ICP–MS without dynamic reaction or collision cell. The sample located in the ablation chamber is hit by a laser beam schematically shown in grey. Detailed description of various LA–ICPMS components is provided in the text.

insufficient energy density (irradiance below the ablation threshold value), and the sample may crack or break out. Such "non-ideal" and variable ablation conditions produce more large particles, and their presence in the aerosol is considered to be a primary cause for elemental fractionation (outlined below). Laser beams with a homogeneous energy density allow for the analysis of standards and unknowns with identical laser-ablation conditions and with variable pit sizes to optimize the analytical resolution on the samples. Moreover, because uniform sample layers are ablated, the resulting pit has a flat-bottomed pan shape, and depth profiling with a sub-micrometre resolution becomes feasible.

Laser pulse duration is essential, because the irradiance increases with decreasing pulse duration for a given laser fluence. Short pulse durations allow for less heat dissipation into the matrix and, consequently, a larger fraction of sample material is vaporized (modeled by Bogaerts & Chen 2005). Present day commercial laser-ablation systems are predominantly equipped with lasers producing nanosecond pulses. Solid source lasers, *e.g.*, the Nd–YAG lasers, are characterized by a pulse duration of *ca*. 5 ns, while excimer lasers produce somewhat longer pulses of *ca*. 20 ns. Laser pulse duration appears to be a parameter of subordinate importance for the analysis of silicates and oxides relative to metals, however, when the irradiance is clearly above the ablation threshold values for all matrices to be analyzed. Therefore, nanosecond laser sources are perfectly suitable for most geochemical applications (*e.g.*, Günther & Hattendorf 2005).

Laser wavelength is a key parameter simply because laser beam coupling with any given matrix strongly depends on laser wavelength, *i.e.*, monochromatic light absorbance and reflectivity vary with wavelength and target matrix. Historically, almost all available wavelengths (*e.g.*, 694 nm, Gray *et al.* 1985; 1064 nm, Jackson *et al.* 1992; 266 nm, Jenner *et al.* 1993) have been used for LA–ICP–MS, but research soon demonstrated that shorter wavelengths (notably 213 nm quintupled Nd–YAG and 193 nm ArF excimer lasers) are more suitable for geochemical applications when using ns-pulsed lasers (*e.g.*, Jeffries *et al.* 1996, Günther *et al.* 1997, Guillong *et al.* 2003a). This is because shorter wavelengths generally couple better with silicates and other transparent materials; hence, the volume affected by a given laser pulse is reduced and thus the energy density in the affected material increased. Although this reduces the ablation rate, the aerosol produced can be processed better by the ICP, resulting in accuracy improvements and lower LOD (*e.g.*, Guillong *et al.* 2003a). Because of the ease of operation of commercially available ns-pulsed UV lasers down to 193 nm wavelength together with their demonstrated performance on silicate and oxide matrices, most LA–ICP–MS geochemical labs currently acquire systems with either 213 or 193 nm laser sources.

<u>Elemental fractionation</u> refers to the changes of element responses (*i.e.*, element sensitivity ratios) with changing LA–ICP–MS analytical conditions (*e.g.*, Longerich *et al.* 1996b). The first parameterization of fractionation was proposed by Fryer *et al*. (1995) who demonstrated for a long transient (*i.e.*, time-resolved) signal from one analytical spot that integrating the first and the second half of the signal and normalizing the resulting intensities with that of Ca does not provide the same values. It implies that sensitivity ratios may evolve with progressive laser drilling at a single spot. Consequently, results for samples may vary as a function of where the signal integration interval is set (*i.e.*, across the entire recorded signal or only across a part of this signal). It has been shown repeatedly in the literature since then, that this type of elemental fractionation can be controlled for various LA–ICP–MS systems when ablation pits are not drilled too deeply. As a rule of thumb, ablations with pit depth to diameter ratios (pit aspect ratios) of less than about two should not suffer from such fractionation with ablation depth (*e.g.,* Borisov *et al.* 2000), again keeping in mind that the extent of this phenomenon strongly depends on LA–ICP–MS setup and operating parameters.

The latest progress in fundamental research on elemental fractionation has identified different locations where fractionation occurs, has constrained their relative importance, and has provided possible processes that cause them. Elemental fractionation relates to processes occurring (i) at the ablation site (aerosol particle size distribution), (ii) during aerosol transport (aerosol sorting effects related to particle size, accepting that the chemical composition of aerosol particles may vary with particle size) and, importantly, (iii) during ionization in the ICP–MS (as reviewed by Günther & Hattendorf 2005). Only very recently, it has become accepted that processes in the ICP fundamentally affect overall element fractionation, and these processes directly relate to the particle size and particle size distribution of the aerosol, which in turn influences aerosol transport phenomena. Additionally, the mass of aerosol per unit time reaching the plasma may be an important parameter, notably for solid state rf generators as commonly used in commercial instruments. All these and possibly other yet unidentified parameters interact to produce elemental fractionation — so, what can we do to fundamentally minimize this problem for geochemical applications?

<u>Aerosol particle size</u>: ideally, every aerosol particle arriving in the ICP is completely vaporized, atomized, and all the atoms are ionized. Reality has shown, however, that this is not necessarily the case. Each aerosol cloud produced by laser ablation is characterized by a particle size distribution, *i.e.*, the range and abundances in particle size fractions. These two parameters have been shown to be highly variable for different laser-ablation conditions and setups.

Evidence that large particles may not be quantitatively ionized comes from different experimental results. Removal of large particles from the aerosol does not result in a proportional signal reduction, suggesting that large particles are not quantitatively ionized in the ICP–MS (Guillong & Günther 2002, Guillong *et al.* 2003b). High-speed digital photography demonstrates that large particles indeed may at least partially survive transit through the ICP without being completely broken down and ionized (Aeschliman *et al.* 2003). Particle size fractions of the total aerosol generated with a 266 nm laser system have been shown to be chemically variable (Kuhn & Günther 2004). Incomplete vaporization of large particles preferentially liberates volatile compounds relative to refractory compounds, according to their vaporization indices. Results from copper isotope measurements by laser ablation – multiple collector ICP–MS have suggested that isotope fractionation is smallest for smallest possible particle sizes (Jackson & Günther 2003). In summary, to minimize elemental fractionation in the ICP it is best to optimize the ablation process so that the smallest possible particle size with a narrow size distribution is produced. The largest mass of silicate particles produced by an energy-homogenized 193 nm LA–ICP–MS system from silicate glass has a particle size below *ca*. 200 nm (Guillong *et al*. 2003a), and these particles appear to be ionized completely in commercially available ICP–MS instruments run at robust plasma conditions (see below).

Controlled ablation of any matrix only occurs well above the ablation energy threshold. It is therefore essential that there is enough energy at any site in the ablation pit in order to ablate the sample properly. This may not be ensured for laser systems that do not have a homogenized energy distribution at the ablation spot but simply focus their Gaussian energy distribution emitted from the laser source onto the sample surface. Ablation near the threshold energy tends to be less well controlled, showing splintering and producing poorly defined rims of ablation craters. It is intuitive that such catastrophic ablation conditions form much larger, and many more, large particles. Hence, avoiding such uncontrolled ablation conditions near the laser-ablation threshold irradiance will considerably reduce elemental fractionation.

The ablation chamber gas environment strongly affects the resulting aerosol characteristics, too. Improved sensitivities for a nanosecond-pulsed LA–ICP–MS setup by using He as the ablation chamber gas instead of Ar (Eggins *et al.* 1998) probably relate to reduced deposition of particles around the ablation pit. The aerosol plume above the ablation pit may expand more freely in He when compared to Ar, thus reducing the probability of material condensation to large particles that may get deposited in the aerosol transport system. Therefore, the observed improvement in sensitivity when using He in the ablation chamber and keeping all other parameters constant probably relates to the transport of a larger mass of smaller particles to the ICP–MS.

Future LA–ICP–MS developments**:** In summary, a nanosecond-pulsed laser-ablation system providing homogeneous energy distribution across the entire pit and sufficient output energy to ablate all matrices of interest in a controlled manner appears to be currently the best choice from commercially available systems for the analysis of complex geological samples, with 193 nm as the most appropriate wavelength for silicate and oxide matrices (Günther & Hattendorf 2005). The future will show how well such samples are treated by currently much more expensive and more difficult-to-control picosecond or femtosecond laser sources available with various laser wavelengths. The pulse duration of these laser sources can be shorter than the reaction time of the target to the applied energy, *i.e.*, the laser energy can almost fully be deposited into the target material before the plasma plume above the ablation spot starts to form (it forms only after a few ns of irradiance; *e.g.*, Bogaerts & Chen 2005). As a consequence, plasma shielding, the absorption of a considerable amount of laser pulse energy by the evolving plasma above the spot, is virtually eliminated, and the sample irradiance is much higher. This may lead to an ablation process controlled by photo-physical bond breaking instead of melting, boiling and vaporization that is probably the dominant process in ns-pulsed laser ablation (*e.g.,* Russo *et al.* 2004). Such a change in predominant laser ablation processes may significantly reduce elemental fractionation and matrix dependence (*e.g.,* Poitrasson *et al.* 2003). Hence, the potential of picosecond and femtosecond-pulsed laser technology for LA–ICP–MS applications in the geosciences is really promising.

Optimization strategy of the ICP–MS for laser-ablation applications

The sample aerosol arriving at the plasma site of an ICP–MS instrument is vaporized, atomized and ionized; and the ions are extracted by differential underpressure through the interface, focused, filtered according to their mass-to-charge ratio and finally detected. As outlined above, it is best when the aerosol arriving at the ICP is ionized completely. Experiments have identified that this may only be approached for "***robust plasma conditions***", conditions at which fractionation effects resulting from incomplete ionization are minimized. Traditionally, ICP–MS operating conditions have been optimized for low oxide-production rates (plasma temperature-sensitive species, monitored by Th/ThO intensity ratios to be <0.5%) and maximum signal-to-noise ratio for the ions of interest. Günther & Hattendorf (2005) have summarized in detail that other optimization criteria are required to ensure robust plasma conditions. For example, the intensity ratio of U/Th, two elements with nearly equal first ionization energies, mass, and abundance of major isotopes, should correspond to the concentration ratio in the reference material. The silicate glass standard SRM610 from NIST contains 461 µg/g U and 457 µg/g Th, respectively; hence, robust plasma conditions should result in a ^{238}U/^{232}Th intensity ratio of one. Optimizing an ICP–MS instrument to Th/ThO <0.5% and maximum signal/noise ratio of analytes may well result in U/Th ratios much higher than one (Fig. 2 in Günther & Hattendorf 2005). Analyzing samples with such an ICP–MS setting bears considerable danger that aerosol particles are not completely converted into ions. If so, the ionization rate in the ICP will be variable at least for some elements (refractory or non-volatile ones) as a function of sample matrix, and one of the most important advantages of LA–ICP–MS is lost, namely the matrix-independent calibration. The possibility of matrix-independent calibration was demonstrated for silicates by Jackson *et al.* (1992), aqueous fluids from inclusions (Günther *et al.* 1998, Heinrich *et al.* 2003), oxides (*e.g.,* Heinrich *et al.* 2003), carbonates (*e.g.,* Eggins *et al.* 2003) and even for Fe, Ni, Co and Cu in some sulfides (chalcopyrite, pyrrhotite and millerite; Halter *et al.* 2004a). Therefore, unless we employ matrix-matched calibration, the careful analyst has to ensure robust plasma conditions for the variable matrices as commonly analyzed in geochemistry.

***Representative recording of fast, transient signals*:** The analysis of entire, crystallized silicate MI by LA–ICP–MS aims at correctly recording cation signals from a mixture of small phases (Fig. 3-4), including silicate, oxide and phosphate minerals, and possibly a volatile phase present in the bubble. For sulfide and carbonate melts, crystallites will vary in composition accordingly. As a consequence, minor and trace elements may become strongly enriched in any tiny phase in the crystallized inclusion. Signals produced from such small phases (*e.g.,* fluid bubbles or accessory minerals in silicate MI or noble metal nuggets in sulfide MI) may be highly transient, notably for very small volume ablation chambers. Pettke *et al.* (2000) have illustrated and discussed causes and effects of non-representative recording of such fast signals in detail. Of quintessential importance is that the transient intensity structure of the signal is defined correctly by all the isotopes of interest in sequential recording mode. This requires short (10 ms or less) dwell times (duration of analysis per isotope in one sweep, where a sweep consists of one sequential analysis of all isotopes of interest) for routines analyzing many isotopes (*e.g.,* >20) as commonly employed in bulk MI LA–ICP–MS analysis. Consequently, the analyst has to know the transient signal intensity curve and duration of a single pulse ablation for the LA setup used (*i.e.*, the signal dispersion of the aerosol transport system) and the number of isotopes to be measured. This allows one to establish compromise conditions between fast scanning protocols, to ensure proper recording of

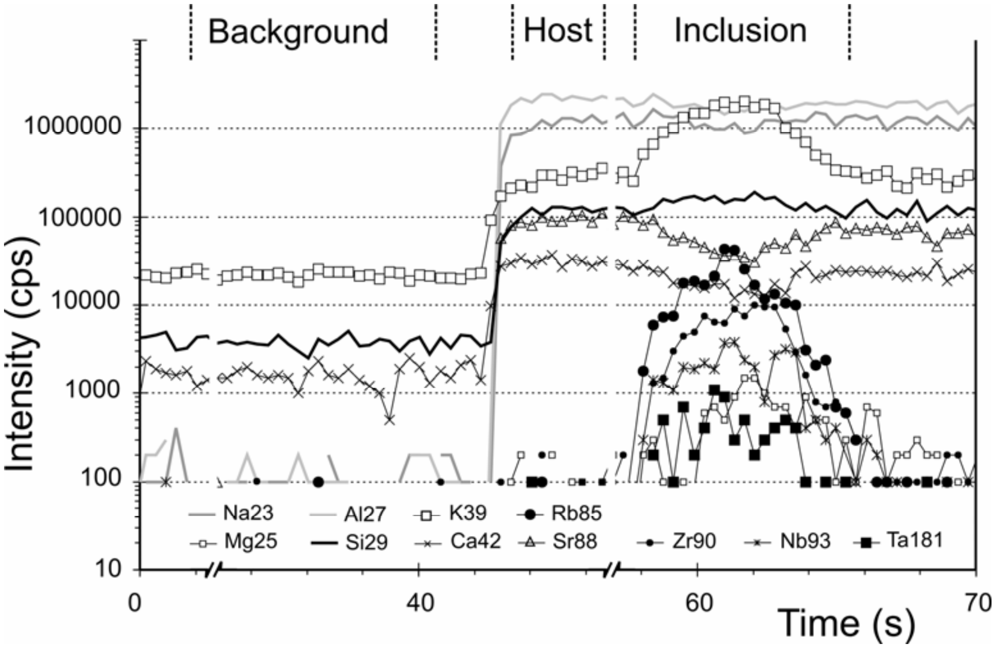

FIG. 3-4: Typical transient LA–ICP–MS signal of a crystallized melt inclusion in plagioclase analyzed in bulk. Note the non-parallel evolution of the inclusion signal interval, *e.g.*, for Rb and Mg, reflecting the ablation of phases enriched in these elements. Elements enriched in the host (*e.g.*, Ca and Sr) display a signal depression in the inclusion interval. Even such elements can be quantified in bulk MI, albeit at lower precision as explained in text.

short transient signals, and slow scanning protocols, since long dwell times lower the LOD when keeping all other parameters constant. Another possibility of extending signals from small crystallites is to use large volume aerosol transport systems. This extends a given signal across a longer time span, thus resulting in lower signal to noise ratios that translate into higher LOD. Therefore, this is not considered to be a viable alternative for bulk MI LA–ICP–MS analysis.

The concern of representative sampling of such short transient signals (Pettke *et al.* 2000) from tiny phases within crystallized MI may be relaxed by at least partially homogenizing the inclusions of interest. For volatile-rich inclusions, this procedure always bears the danger of decrepitation during atmospheric heating (*e.g.,* Student & Bodnar 2004). Moreover, partial homogenization of MI is no guarantee that the content of tiny daughter crystals has become homogeneously distributed throughout the entire MI. Probably the most reliable test for representative sampling of elements exclusively contained in tiny daughter crystals is the external (*i.e.*, inclusion-to-inclusion) reproducibility achieved for element concentrations in a MI assemblage. For signals not limited by counting statistics uncertainty, the uncertainty of average assemblage element concentrations should be uniform.

Mass interferences may also plague LA–ICP–MS analysis. Among them, plasma gas based interferences are properly accounted for by background subtraction. Isobaric interferences (*e.g.*, $^{58}\mathrm{Fe}^+$ on $^{58}\mathrm{Ni}^+$, being the most abundant Ni isotope) can largely be avoided by proper mass selection (for Ni in Ca-rich matrices this is $^{62}\mathrm{Ni}$ because of $(^{44}\mathrm{Ca}^{16}\mathrm{O})^+$ on $^{60}\mathrm{Ni}^+$) and accepting higher LOD. Alternatively, isobaric overlap can be corrected mathematically, after analysis, based on known isotopic abundances of interfering elements. Problematic interferences are polyatomic ions that form by combination of elements abundant in the plasma gas with elements abundant in the analyzed matrix. Such “dangerous” polyatomic ions include all the element oxides (simply because oxygen is the most abundant element in silicates) or, more specifically, $(^{27}\mathrm{Al}^{16}\mathrm{O})^+$ and $(^{28}\mathrm{Si}^{16}\mathrm{O})^+$ on $^{43}\mathrm{Ca}^+$ and $^{44}\mathrm{Ca}^+$ (many major silicates); metal argides, $(\mathrm{M}^{40}\mathrm{Ar})^+$, *e.g.,* transition metal argides on Rb, Sr, Zr, Nb, Mo, Ru, Rh or Pd or $(^{23}\mathrm{Na}^{40}\mathrm{Ar})^+$ on $^{63}\mathrm{Cu}^+$; or simply pure matrix-sourced interferences, *e.g.,* $(^{16}\mathrm{O}^{16}\mathrm{O})^+$ or $(^{16}\mathrm{O}^{18}\mathrm{O})^+$ on $^{32}\mathrm{S}^+$ and $^{34}\mathrm{S}^+$, respectively; $(^{40}\mathrm{Ca}^{12}\mathrm{C})^+$ on $^{52}\mathrm{Cr}^+$ in carbonates; or $(^{56}\mathrm{Fe}^{32}\mathrm{S})^+$ on $^{88}\mathrm{Sr}^+$ in iron sulfides. For some of these, dynamic reaction cell or collision cell ICP–MS technologies coupled with laser ablation may reduce the problem significantly (*e.g.,* Hattendorf & Günther, 2000). Doubly charged ions may also interfere, *e.g.,* $^{138}\mathrm{Ba}^{++}$ on $^{69}\mathrm{Ga}^+$ (recall that the mass filter of an ICP–MS resolves ions according to their mass/charge ratio). The mass resolution of quadrupole instruments is commonly insufficient to resolve all these types of interferences. Magnetic sector field instruments have tunable resolution and are thus capable of resolving some of these interferences; yet, increasing the mass resolution inevitably lowers the sensitivity, and consequently LOD are compromised. And only recently, sector field instruments have become fast enough for transient signal recording from inclusions (*e.g.,* Latkoczy *et al.* 2002). They are still considerably slower than quadrupole instruments, however, and thus not the instrument of choice for recording of isotopes across the entire mass range (Li to U) of fast transient signals produced from MI ablation.

Limits of detection are a key parameter in LA–ICP–MS applications, notably for the analysis of inclusions where the sample mass available for analysis is limited. The ablated mass of sample per unit time exerts the dominant control on the resulting LOD from the laser ablation side. For spot analyses of a homogeneous phase using a 193 nm excimer laser, the LOD very roughly decreases by a factor of 4 when doubling the pit diameter. Additionally, aerosol dispersion (dominantly in the ablation chamber volume, less importantly in the transport tubing) prior to entering the ICP leads to reduced signal/background ratios for short transient signals (a given signal is smeared over a longer time), resulting in lower element sensitivities and thus higher LOD. Therefore, small volume aerosol transport systems (notably the ablation chamber) will increase the signal/background ratios for a given mass of sample as available for inclusion analysis and thus minimize the LOD. However, for minimized signal duration (resulting in highest signal/background ratios) the requirement of representative signal recording introduced above has to be properly accounted for. The laser energy density used on the sample is of subordinate importance here, provided it is clearly above the ablation threshold. The recommendations by Longerich *et al.* (1996a) for the calculation of LOD reveal that the quality of recording the gas background (*i.e.*, the scatter of the background measurement) most prominently influences the resulting LOD from the ICP–MS side. LOD values are only useful numbers for known LA–ICP–MS parameters and LOD filtering criteria. LOD using the 3 sigma criterion (Longerich *et al.* 1996a) can be as good as single µg/g values for elements from the middle to heavy mass range when analyzing a homogeneous phase with a pit of 80 µm and 10 Hz laser repetition rate in single spot or raster mode. For bulk MI analysis drilled out of the host mineral, resulting LOD are between a few thousand µg/g and several tens of ng/g, depending primarily on the isotope analyzed, MI size, ablation quality and element compatibility in the host (compare Fig. 12 in Heinrich *et al.* 2003, for LOD estimates in 25 µm inclusions). When analyzing bulk MI, best LOD values are achieved for elements incompatible in the host mineral, with fast drilling and with 30–50 µm spherical MI. Larger MI do not allow for better LOD values when analyzed in bulk because the reconstruction of the pure MI from the mixed signal is the limiting factor.

In summary, accurate LA–ICP–MS measurements of geological materials including multiphase inclusions in minerals should follow the philosophy of keeping all parameters as uniform as possible in order to reduce the potential for complications. This approach requires:

- enough laser energy density on the sample to ablate all matrices of interest in a controlled manner,
- homogenized energy distribution across the ablation pit, to minimize energy-density-dependent changes in aerosol production (notably aerosol particle size) and to control the ablation process,
- laser ablation in He to maximize analytical sensitivity,
- robust plasma conditions, to minimize ICP–MS–induced element fractionation, and to provide matrix-independent external calibration,
- low and constant gas backgrounds to achieve low LOD,
- representative recording of short transient signals, not to (partially) miss trace elements enriched in tiny crystallites or in exsolved fluid bubbles, and
- keeping interferences in mind for proper analyte isotope selection, notably matrix-based polyatomic interferences.

Obviously, if the analysis of entire MI drilled out of the host mineral is accurate, the measurement of exposed glassy MI by spot analysis poses no additional problem.

ANALYSIS AND DATA QUANTIFICATION STRATEGIES OF MI BY EPMA, SIMS, RAMAN AND LA–ICP–MS

The most important difference between the analysis of MI by EPMA, SIMS, Raman, FTIR and LA–ICP–MS is that with all the former techniques only a tiny fraction of the total MI mass can be measured, while LA–ICP–MS also has the capability of analyzing an entire inclusion. Consequently, for all analytical approaches not analyzing the entire inclusion the analyzed mass of sample must be representative of the bulk MI composition. It requires that reversible post-entrapment modifications are indeed accurately corrected in the lab prior to analysis. For MI that cannot be homogenized in the lab at entrapment P, T, for example, due to volatile loss as commonly observed in hydrous volcano-plutonic rocks, LA–ICP–MS currently remains as the only microbeam technique for chemical analysis. The same is true for sulfide MI that hardly ever quench to a homogeneous glass (Halter *et al.* 2002b, 2004a, 2005, Halter & Heinrich 2006). The data-reduction scheme for LA–ICP–MS bulk MI analyses outlined below will demonstrate that multiphase (*i.e.*, partially crystallized) MI can be accurately (Pettke *et al.* 2004, Halter *et al.* 2004a) quantified, including the fraction of post-entrapment (sidewall) crystallization.

Signal quantification strategies

All microbeam techniques are relative analytical methods, *i.e.*, the instrument response needs to be calibrated against standards of known element abundances. This external standardization is best done with matrix matching the sample material; for EPMA it is important and for SIMS it is a prerequisite. Matrix-dependence of analyte signals may also be corrected for by establishing matrix-dependent calibration curves, *e.g.*, as done for the analysis of volatile species by vibrational spectroscopy techniques. FTIR (*e.g.*, Stolper 1982, Newman *et al.* 1986) analysis achieves LOD for H and C bearing species similar to those obtained by SIMS, at similar spatial resolution (*e.g.*, Hauri *et al.* 2002), and the analysis of water in silicate glasses of a wide compositional and structural range has become possible by confocal Raman microprobe (Zajacz *et al.* 2005). The aim of standardization for all these techniques is to determine the sensitivity of the elements on an external standard (*i.e.*, the amount of signal per unit time and concentration, *e.g.*, counts per second per µg/g) and to analyze the sample at identical instrument conditions. Provided that signal intensity variations are generated exclusively by variable analyte concentrations, element concentrations in the sample are uniquely defined by the use of external standardization alone.

For the case where analyte signal intensities change in response to variables other than analyte concentrations, external standardization alone fails to quantify a measurement. Such additional variables may include (a) chemical and structural differences in matrices between external standard and sample, (b) differences in analytical conditions, *e.g.*, variable beam size, between external standard and sample or (c) variability in sample introduction, *e.g.*, non-uniform flushing of the ablation chamber in LA–ICP–MS. If the sum of this additional variability results in a *uniform* signal intensity change, an intensity shift at constant element sensitivity ratios, independent knowledge of one element concentration in the sample is sufficient to quantify such signals. This element is named the internal standard and is used to determine the relative sensitivity factor, unique for every analytical spot, between external standard and sample. Combined external and internal standardization is vital for the quantification of LA–ICP–MS data (*e.g.*, Longerich *et al.* 1996a).

The condition of variable signal intensities at constant analyte sensitivity ratios just described may not be fulfilled in some cases. For example, the analyte sensitivity ratios can vary with changing matrix chemistry or changing analytical conditions, *e.g.*, beam size or duration of drilling in LA–ICP–MS, or both. For an analytical setup where element sensitivity ratios vary between measurements on the external standard and the sample, the only way of getting accurate data is strictly matched analytical conditions to eliminate such variability. Most commonly, the matrix between external standard and sample is matched. This matrix-matched calibration is essential for EPMA and vital for SIMS. For both techniques, other instrumental parameters are kept strictly uniform between standard and sample analysis.

These considerations illustrate the potential problems we encounter for MI analysis. The simplest case is glassy silicate MI exposed on the sample surface. Matrix-matched standardization at uniform beam size is easily ensured for any of the microbeam techniques. The analysis of multiphase (crystallized) MI is more complex. Different matrices are all analyzed at once, requiring matrix-independent analytical conditions for LA–ICP–MS (*i.e.*, robust plasma conditions). And the entire MI needs to be analyzed in order to reconstitute its chemical composition at the time of trapping. In order to optimize the MI-to-host-mineral mixing proportion during LA–ICP–MS MI analysis, the laser beam size needs to be adjusted for every inclusion, thus requiring beam size-independent external calibration. The analyst is therefore confronted with a large extent of "mismatch" between analytical conditions used for the measurement of external standards and MI samples. This required flexibility in sample-related parameters holds much potential for inaccurate analysis. Therefore, an approach for the accurate analysis of entire MI drilled out of the host mineral using LA–ICP–MS is outlined now.

LA–ICP–MS bulk MI analysis

The bulk analysis of MI (be they crystallized or glassy) by LA–ICP–MS is schematically shown in Fig. 3-5. Data recording by the ICP–MS is started to acquire the gas background signal. After ~50 s, the laser is switched on and drills first through the host mineral, then hits the inclusion, and the laser is switched off only when the entire MI is consumed. Data recording is stopped. The detailed mathematical formulation for quantification of such signals including a rigorous uncertainty assessment is provided in Halter *et al.* (2002a); hence, only the conceptual approach behind the quantification strategy is described here. The analytical signal consists of a pure host mineral interval and an inclusion interval representing an *a priori* unknown mixture between host and inclusion contribution. Quantification of the MI composition thus requires two steps. The two signal intervals, host mineral and inclusion plus host mixture, must be quantified first. Bracketing external standardization (commonly done using SRM61X glasses from NIST) determines the instrument responses for all analytes and corrects linearly for instrument drift. These element responses are then converted to concentration data for the two signal intervals simply by normalizing the element abundances to a fixed element–oxide total (*e.g.*, Leach & Hieftje, 2000), *i.e.*, the sum of all element oxides measured (commonly 100 wt.% minus the amount of non-analyzed volatiles such as H_2O). This quantification step is straightforward,

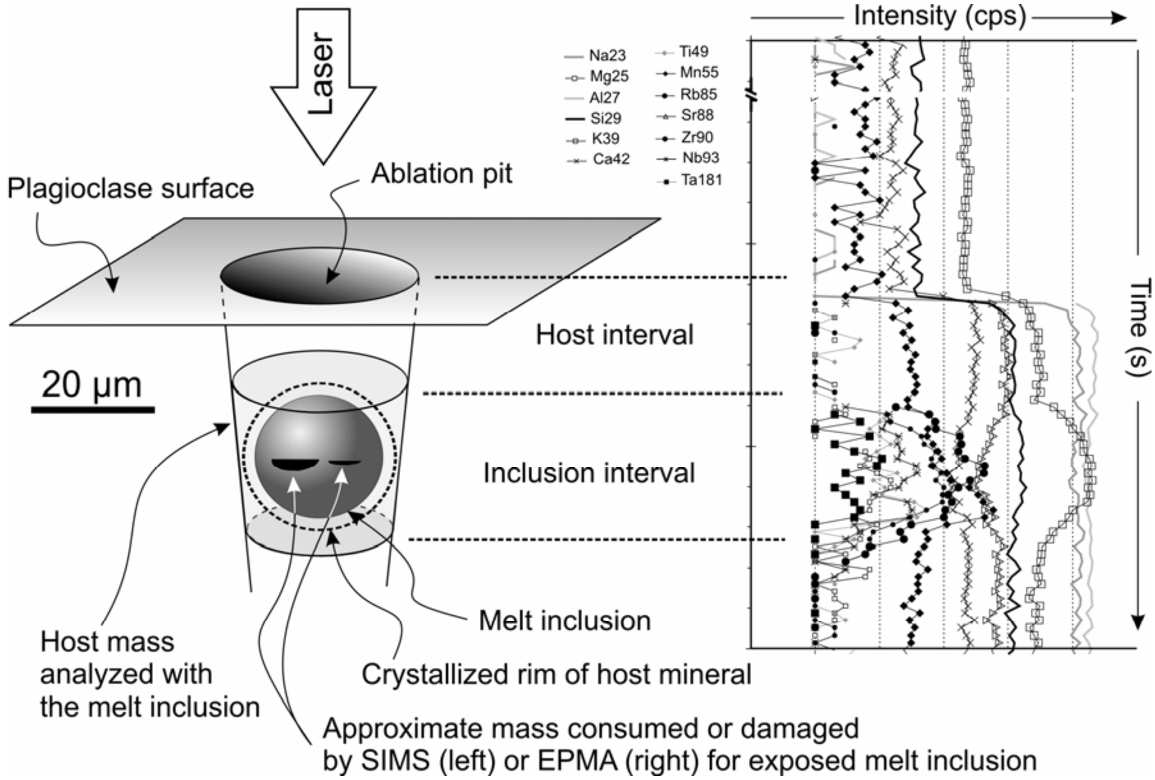

FIG. 3-5: Schematic representation of the LA–ICP–MS analysis of an entire melt inclusion (MI) modified from Halter *et al*. (2002a), with the resulting signal for a MI in plagioclase shown to the right. The approximate mass consumed or damaged for analysis by EPMA or SIMS is shown in black for comparison.

following the procedure detailed in Longerich *et al*. (1996a).

The second step is then to unmix the inclusion signal from the host signal, *i.e.*, to determine the ratio between the mass of the MI and the total mass of the ablated inclusion interval (Fig. 3-6). This ratio, which is unique for every MI analysis, can be calculated provided that a second constraint is available:

(i) The concentration of one element in the melt at the time of inclusion entrapment is known. Ideally, this element is abundant in the melt and scarce in the host.
(ii) The concentration ratio of an element pair present in the melt at the time of inclusion entrapment is known. Again, such a ratio in the melt should be very different from that in the host.
(iii) The mass ratio between inclusion and host for the signal interval is known independently.

This second constraint together with the pure host mineral composition then allows the calculation of the pure MI composition by subtracting the appropriate amount of host mineral from the mixed signal. Obviously, the accuracy of inclusion composition primarily depends on the quality of this second constraint.

Various approaches exist for determining this second constraint for LA–ICP–MS MI quantification.

- MI are homogenized in the lab and then measured for their major element composition by EPMA. These results can then be used as an internal standard for the bulk MI analysis and the spot analysis of exposed glassy inclusions.
- A series of bulk-rock compositions from a magmatic complex define the range in magma composition with progressive magma evolution. Provided that one element concentration remains essentially invariable throughout, it may be used as an internal standard. In evolved volcano-plutonic centers at convergent margins, bulk Al_2O_3 can commonly be used (Halter *et al.* 2002a, Audétat & Pettke, 2003).
- This last approach can be refined by comparing bulk rock element correlation plots with the superposed mixing line for the inclusion–host mixed signal interval (Fig. 3-6). By incrementally

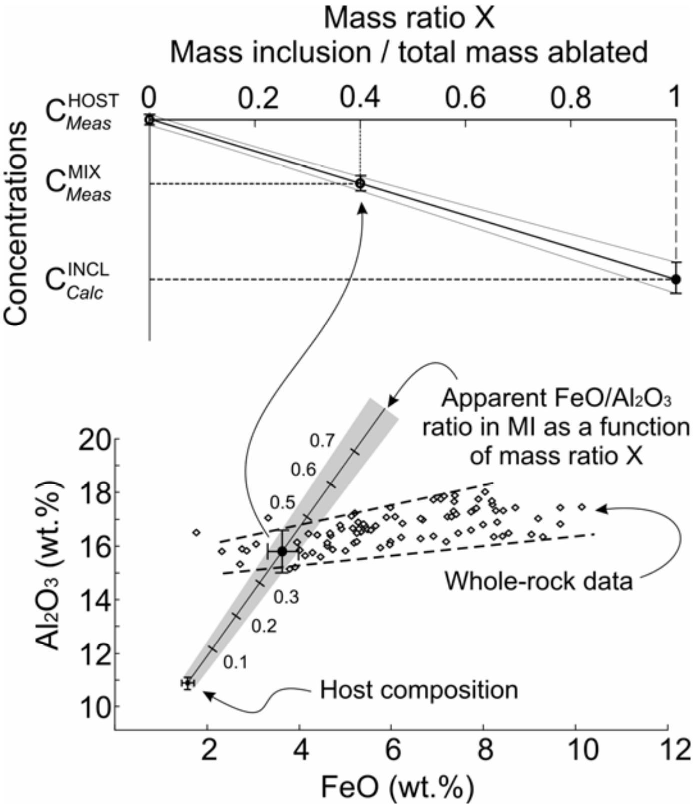

FIG. 3-6: Schematic illustration of LA–ICP–MS bulk melt inclusion (MI) signal quantification based on the determination of the mass ratio between inclusion and the total mass ablated in the inclusion signal interval (compare Fig. 3-5). The constraint to calculate the mass ratio between inclusion and total mass ablated in the inclusion interval is defined by the intersection of the trend in FeO/Al$_2$O$_3$ concentration ratio of the MI obtained via incrementally subtracting host mineral component from the mixed signal interval with the trend in whole rock data. See text for explanations.

varying the ratio of inclusion mass divided by total mass ablated for the inclusion signal interval, we obtain a line defined by apparent melt compositions as a function of MI–host mixing proportions. The intersection of this line with the correlation line of the bulk rock data then defines the correct mass ratio for this inclusion signal interval (Halter *et al.* 2002a), assuming that MI and bulk rock have similar element concentration ratios.

- Any internal standard derived from bulk rock element concentrations does not take into account the elements fixed in phenocrysts at the time of MI trapping. Notably for MI trapped at high rock crystallinity, the best way of estimating an element concentration in the original MI is to forward model the chemical evolution of residual melt in the rock relative to the crystallinity estimated for the time of MI entrapment.
- Use published element distribution coefficients between host mineral and melt at entrapment conditions, and calculate the element concentration in the melt based on that measured for the host mineral in the same analysis.
- Inverse modeling of rock crystallization (starting from matrix-glass data) and of host mineral crystallization from the MI onto inclusion walls should result in an intersection of trends that defines the element concentrations at the time of MI entrapment (Pettke *et al.* 2004).
- Determine volumetric proportions between MI and the host mineral in the mixed signal interval (Fig. 3-5) optically and convert this to the mass ratio between the two. This last option has turned out to be not precise enough (Halter *et al.* 2002a); hence, it is not considered further.

The above considerations shall serve as a conceptual approach on how to derive an internal standard for the quantification of LA–ICP–MS bulk MI data. What follows is a discussion about advantages, complications and limitations of this bulk MI approach by LA–ICP–MS.

This LA–ICP–MS data reduction scheme automatically corrects for the fraction of host mineral crystallized onto the inclusion walls after entrapment. Therefore, it is not necessary to know the amount of post-entrapment crystallization onto the inclusion walls nor is it required to re-melt this rim of crystallized host into the melt prior to bulk MI analysis by LA–ICP–MS.

The quality of this internal standard is obviously key to the accuracy of the MI composition. First of all, relevant data may not be available, *e.g.*, element distribution coefficients at P and T for the magma of interest, or data bases for modeling the reverse of host mineral crystallization out of the trapped MI may not be adequate for some host minerals (*e.g.*, Kress & Ghiorso, 2004). Pettke *et al*. (2004) have mathematically explored the effects of inappropriate internal standardization for LA–ICP–MS MI analyses. An apparently simple sample of glassy MI from a dredged MORB sample (Fig. 3-2B) was used for this purpose. The various scenarios presented in Pettke *et al*. (2004) illustrate well that MI concentrations may be overestimated or underestimated, and it is intuitive that inaccurate host mineral subtraction affects elements compatible in the host less than those incompatible in the host. The variability of results exceeded 20% (*e.g.*, $7.68 < \text{MgO} < 9.42$) even for the petrographically pristine MI in a fresh, dredged MORB sample (Fig. 3-2B) containing less than *ca*. 15% phenocrysts. Impressive for this case is the degree of post-entrapment crystallization onto the inclusion walls – it amounted to 11 wt.% on average. It is fair to state that for the complex case of MI from strongly evolving systems, the danger for inappropriate internal standardization needs to be taken seriously. The most robust check on the possibility of inappropriate standardization is to apply a variety of internal standards for MI data reduction, to explore their effects on the final result.

STATISTICAL RELEVANCE OF DATA SETS GENERATED FROM LA–ICP–MS, SIMS AND EPMA ANALYSIS

The type of geochemical problem to be solved defines the required precision of the analytical data set. Two basic types of data sets need clear distinction. Data for individual inclusions with associated analytical uncertainty may either represent a single spot analysis (internal precision; where available) or averaged multiple spot analyses obtained on a single inclusion (external precision). Alternatively, averages may be calculated from the analysis of several individual inclusions belonging to a MI assemblage. The resulting inclusion-to-inclusion reproducibility should not exceed analytical scatter as indicated by mean square weighted deviates (MSWD) values for MI assemblages (Pettke *et al.* 2004, and further below).

The best possible analytical precision at high spatial resolution for individual spot measurements of MI is required to check for homogeneity of reheated inclusions (using multiple spots on individual inclusions). Heterogeneities within petrographic MI assemblages can be explored by highly precise spot analyses of several inclusions from one assemblage in order to constrain MI entrapment processes (*e.g.*, equilibrium *vs.* disequilibrium entrapment; Faure & Schiano 2005).

Accuracy at useful analytical precision is required to constrain the chemical composition of source melts. Such data obtained on MI of known entrapment history may then be used to trace the chemical evolution of the residual melt in magmatic systems (*e.g.*, Halter *et al.* 2004b) or to investigate element distribution between coexisting phases such as fluid and melt (*e.g.*, Audétat & Pettke 2003). As outlined above and illustrated in Fig. 3-1, the petrographically most reliable definition of MI entrapment sequence is the geometric arrangement of MI assemblages in rock-forming crystals. Average MI assemblage compositions are thus perfectly suited for studying igneous processes. Consequently, the time frame and scale of investigation defines what type of data is ideally used to attack the problems.

The analytical uncertainties associated with data sets obtained by the various microbeam techniques are addressed now. First, it should be appreciated that uncertainties for trace element concentrations of individual spot analyses near the machine-specific LOD are dominated by the uncertainty in counting statistics for all instruments unless instrument backgrounds are large. These uncertainties are easily 50% or more and provide a minimum uncertainty for each element analysis in individual inclusions. Error propagation for LA–ICP–MS analysis of individual MI includes analytical uncertainties on the host mineral and the mixed signal interval (including counting statistics and plasma flicker), and the uncertainty on the extrapolation of MI composition from signal deconvolution of the mixed signal interval (Halter *et al.* 2002a). To my knowledge, a similar propagation of analytical uncertainties is not available for individual spot analyses by EPMA and SIMS. Consequently, the uncertainties on LA–ICP–MS analyses of individual MI allow one to identify "bad" analyses, for example those suffering from dominant host contribution to the mixed signal, and discard them (Halter *et al.* 2002a).

For the case of analyzing entire MI by LA–ICP–MS, additional uncertainty on the MI composition stems from subtraction of the host mineral contribution to the mixed signal. Therefore, LA–ICP–MS data of unexposed MI are less precise than spot analyses of exposed MI by SIMS, EPMA and LA–ICP–MS itself. This additional uncertainty is larger for chemically similar MI-host mineral pairs (*e.g.*, andesitic MI in amphibole; Halter *et al.* 2002a) or, generally, for trace elements enriched in the host, as nicely illustrated for Sr in plagioclase-hosted MI (Halter *et al.* 2002a) or Zr in MI hosted by two chemically distinct clinopyroxene crystals from one rock sample (Pettke *et al.* 2004). Typical uncertainties for individual element concentrations in a bulk LA–ICP–MS MI analysis are between a few percent for elements incompatible in the host and may be as high as a few tens of percent for those dominantly present in the host. Comprehensive data sets including uncertainties of individual bulk MI measurements by LA–ICP–MS are provided elsewhere (*e.g.*, Halter *et al.* 2002a, Pettke *et al.* 2004, Halter *et al.* 2004b). Obviously, the analyst has to strive for maximal inclusion to host mass ratios for the signal interval to minimize uncertainties on MI compositions. Hence, the ablation pit has to be large enough to ablate the entire MI plus crystallized rim of host after entrapment, but as small as possible to minimize the host contribution to the signal interval (Figs. 3-5,6). Therefore, analytical uncertainties on individual bulk MI measurements by LA–ICP–MS need to be quantified, and the detailed formalism to do so is provided in Halter *et al.* (2002a).

Having quantified uncertainties on individual MI measurements then allows us to calculate uncertainty-weighted, average element concentrations for MI assemblages, following the concept that the analyzed MI represent individual samples of a chemically uniform melt at the time of their entrapment (*i.e.*, homogeneous assemblages). This is advantageous because precise analyses exert a larger influence on the resulting average element concentrations than do imprecise ones. This is especially important for element concentrations near their LOD. Moreover, MSWD values can be obtained for uncertainty-weighted averages (commonly employed in isochron dating; *e.g.*, Ludwig *et al.* 1994), serving as a test whether the variability in averaged data sets can be explained by analytical uncertainty alone. If not, initial heterogeneity within the MI assemblage is indicated (illustrated in Pettke *et al.* 2004, and further below).

As there is no generally accepted way of determining element concentration uncertainties on a single spot analysis by SIMS or EPMA, simple multi-spot averages with standard deviation uncertainties are used to assess analytical precision (*i.e.*, the external spot-to-spot reproducibility is used instead of the single spot uncertainty-weighted average as available in LA–ICP–MS bulk MI analysis). This can be done by either averaging multiple spot analyses obtained from a single MI, or by averaging spot analyses from a series of MI of one assemblage. This procedure weights each analytical point equally. A comparison between average MI element concentrations obtained by different analytical methods is shown in Figure 3-7 (data from table 3 in Pettke *et al.* 2004). It can be seen that average concentrations obtained on exposed MI by spot analysis (SIMS and EPMA) largely agree with those obtained on crystallized MI analyzed in bulk by LA–ICP–MS, and that one standard deviation uncertainties are similar for the different analytical techniques employed (Fig. 3-7A). The calculation of uncertainty-weighted average element concentration for the same LA–ICP–MS data set changes the numbers only slightly but results in considerably smaller uncertainties. Comparison of these data with average SIMS and EPMA data (Fig. 3-7B) shows less agreement than between the averaged data shown in Fig. 3-7A. Elements that disagree generally show high MSWD values, indicating sample variability in addition to analytical uncertainty. This suggests that MI from different assemblages with evolving element concentrations were averaged in the current data set. Because different MI were analyzed by the various techniques, the respective average element concentrations of elements present at variable abundances will not overlap. Consequently, uncertainties on uncertainty-weighted average element concentrations will in this case under-estimate the variability of the data set.

Uncertainty-weighted average compositions of MI assemblages determined by LA–ICP–MS are therefore considered to be a very robust determination of the melt chemistry present at various stages during magma evolution. It infers that LA–ICP–MS analysis of entire crystallized MI from assemblages constrains the assemblage bulk composition with analytical precisions (appreciating the statistical differences inherent in the various data sets) similar to those obtained for EPMA and SIMS averages from exposed glassy MI.

STRENGTHS OF THE VARIOUS MICRO-BEAM TECHNIQUES

The following section about key competences of each analytical setup shall illustrate

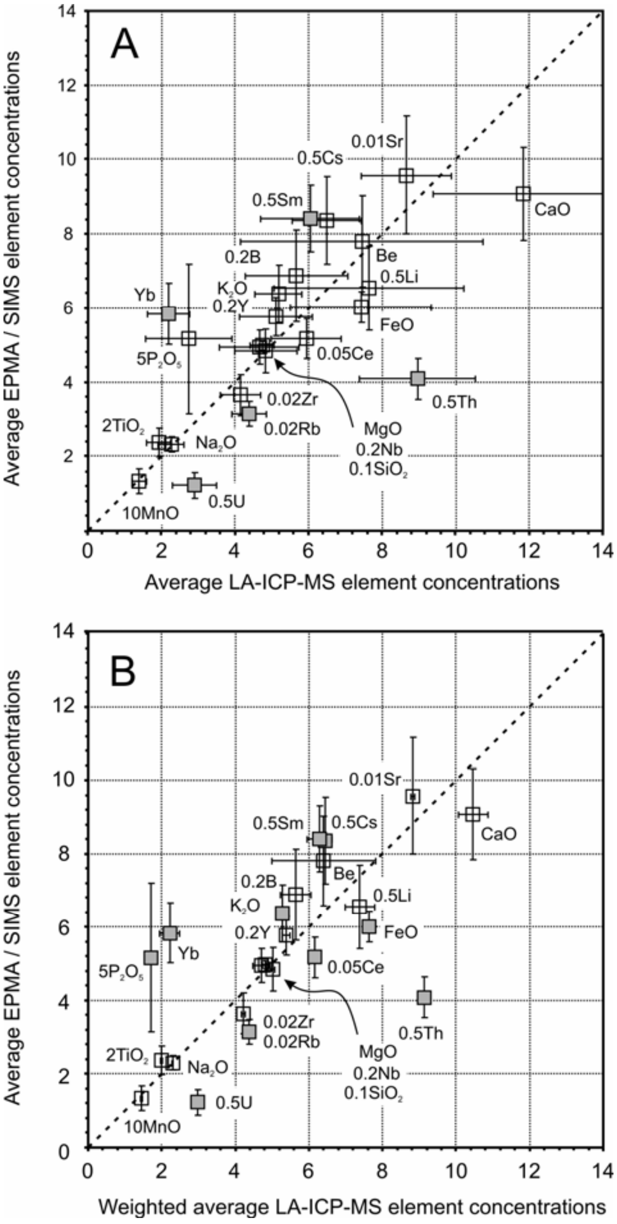

FIG. 3-7: Comparison between average element concentrations determined by secondary ion mass spectrometry (SIMS) or electron probe microanalysis (EPMA) and LA–ICP–MS bulk melt inclusion (MI) data. The MI were hosted in clinopyroxene of a sample from Mt. Somma Vesuvius. Data for each individual inclusion are reported in Pettke *et al*. (2004). Data are expressed in wt.% element oxides or in µg/g for trace elements, and plotted linearly, scaled with the preceding factor as labeled. Figure A compares simple averages obtained for both data sets. Error bars are 1 standard deviation and show that uncertainties in average element concentrations of these MI are comparable between the analytical methods. Elements in gray do not agree within 1SD uncertainty between the methods (the reasons for disagreement are discussed in Pettke *et al.* 2004). Figure B shows the comparison between uncertainty-weighted average MI composition obtained by bulk MI LA–ICP–MS and average SIMS or EPMA data. Again, elements that disagree between the methods are shown in grey. Most of these elements show high MSWD values (reported in table 3 of Pettke *et al.* 2004), indicating that variability in individual MI element concentrations exceeds pure analytical variability. This would imply that MI from different assemblages are averaged in the current data set.

their complementary character. Therefore, the geochemical questions to be attacked will dictate which instrument(s) are ideally employed for analysis.

It is well known that LA–ICP–MS cannot analyze all elements of the periodic system – the notoriously difficult if not impossible elements are those in the upper right corner of the periodic table. The impossible elements are those with a first positive ionization potential higher than that of Ar (*e.g.*, F). Volatiles such as H, N and O are currently not possible either. Sulfur in silicates, carbonates or phosphates, cannot be analyzed on a quadrupole instrument because matrix-based O_2^+ interferences cannot be resolved – high-resolution sector field instruments would be required for this (*e.g.,* Evans *et al.* 2001, Lahaye *et al.* 2004). Because of poor ionization efficiency and elevated background signals, C and Cl may not give useful LOD values in MI. Provided that inclusions can be homogenized reliably in the lab, data for the above elements can be obtained by SIMS and even EPMA with much better detection power.

Volatiles in MI are extremely important because their abundance in melts strongly affects magma dynamics and equilibrium crystallization, and MI are likely to preserve the least modified volatile content of the original melt (*e.g.,* Metrich & Clocchiatti 1989, Grove *et al.* 2002, Wallace 2005). Water is among the most important volatile species, explaining why much effort has been put in its accurate analysis in MI. Applications of FTIR to the analysis of volatile species in MI has been essential in advancing our understanding of volatile contents in melts (*e.g.,* Lowenstern & Mahood 1991, Wallace *et al.* 1999). The main disadvantage of this technique is the need for exposing MI glasses on both sides for measurement by doubly polishing while maintaining sufficient thickness to perform reliable absorbance measurements. SIMS may be used as an alternative analytical technique to FTIR for the analysis of some volatiles, and Layne (2006) addresses this topic. Notably thanks to the introduction of the use of a Cs^+ ion source, allowing for the analysis of negative ions, such volatile elements can now be detected down to µg/g concentrations (*e.g.,* Hauri *et al.* 2002). For the analysis of water in silicate glasses at concentrations of *ca*. 2 wt.% or more, the use of Raman spectroscopy has been explored (*e.g.,* Thomas, 2000). Recently, a novel quantification approach for confocal Raman water measurements has been developed, allowing fast measurements of inclusions of variable composition entirely enclosed in the host mineral (Zajacz *et al.* 2005), at analytical precisions inferior to those obtained by SIMS, however. The fact that MI need not be exposed to the surface for confocal Raman analysis minimizes problems of contamination or exchange between MI glass and ambient air; hence, this technique has great potential for constraining melt water contents particularly when contained in MI. Moreover, as this approach is truly non-destructive, the MI are preserved for analysis by other microbeam techniques.

Analytical resolution is inferior with LA–ICP–MS when compared to the other microbeam techniques. Subtle, small-scale trends in element concentrations are best resolved by EPMA or SIMS, notably for small (<20 µm) inclusions. Such data may be required for example to test for boundary layer problems or diffusional equilibration between the MI and host mineral, *i.e.*, problems where we need precise data at a resolution higher than that achieved with bulk MI LA–ICP–MS (a recent example is provided in Faure & Schiano 2005). A small beam size also allows for multiple spot analyses on one MI to check for homogeneity across the inclusion (serving as a test for the effectivity of homogenization in the lab). SIMS analysis achieves LOD comparable to those obtained with LA–ICP–MS, but consumes much smaller sample amounts, and so SIMS may be the method of choice for small MI. And small MI may be important in constraining mantle melt characteristics (compare Danyushevsky *et al.* 2004). Especially with the advent of nano-SIMS, we may soon have a technique with an analytical resolution hitherto unavailable to the earth sciences (*e.g.,* Stadermann *et al.* 2005, Hellebrand *et al.* 2005).

High resolution chemical imaging can be done with BSE imaging as available in electron probe instruments (*e.g.,* Faure & Schiano 2005), an excellent tool to identify and visualize small scale heterogeneities such as diffusional zoning patterns. SIMS also offers the capability to generate reasonable resolution chemical maps. Such element distribution maps may then be used for designing the next analytical steps.

For EPMA and SIMS analysis, the MI must be exposed at the sample surface. For LA–ICP–MS and confocal Raman analysis, the inclusions may be completely enclosed in the host mineral; hence, many more MI are actually available for measurement in one analytical session (*i.e.*, at one set of instrument optimization). The analysis of all MI at set experimental conditions is essential for precisely constraining average element concentrations for MI assemblages.

LA–ICP–MS is a destructive method, consuming the entire inclusion for bulk MI analysis and thus rendering a revisit impossible. EPMA and SIMS consume or damage much less sample (Fig. 3-5). When diverse analytical techniques are combined, LA–ICP–MS will be done in spot mode on exposed MI. Also in this mode, LA–ICP–MS consumes most sample material. On the other hand, LA–ICP–MS is the only method allowing for analysis of major and trace elements within one analysis (thanks to the dynamic range of ICP–MS detectors of up to 9 orders of magnitude). Consequently, the geologic problem to be solved again determines which instrumental setup is most favorable.

Matrix-matched external standardization at similar concentration levels, which is mandatory for SIMS and recommended for EPMA, is not required for LA–ICP–MS systems operated under the robust plasma conditions detailed above. Therefore, widely used and well-characterized reference materials can be employed for data quantification, improving the comparability of data generated in different labs and thus, ultimately, the reliability of results.

The most efficient tool for determining general chemical characteristics of a series of MI assemblages is LA–ICP–MS, due to the large number of bulk MI analyses obtainable within one analytical session (close to 100 MI plus adjacent host at 20–50 major to trace elements per day). Large data sets from MI assemblages also allow identification and thus exclusion of non-representative MI from further data calculations. Such MI commonly include those having accidentally trapped a solid phase or inclusions of poor analytical quality, *e.g.*, those stemming from non-representative recording of highly transient signals produced from tiny daughter crystals. Robust uncertainty-weighted average compositions of assemblages can thus be obtained from the large LA–ICP–MS data sets. Moreover, each host mineral is measured adjacent to the MI within one analytical shot during identical LA–ICP–MS analytical conditions. This provides a check for host mineral homogeneity (recall that host mineral zoning can be used to identify proper primary MI assemblages), and it allows for the direct determination of element distribution coefficients for major and trace elements alike (recalling limitations imposed by post-entrapment diffusive equilibration).

The above comparison between advantages of the various microbeam techniques for the analysis of MI again emphasizes that the analytical method of choice is dictated by the geochemical problem to be solved. For cases where homogenization of MI to entrapment composition is not possible in the lab, LA–ICP–MS provides the only technique for bulk chemical analysis. In any case, LA–ICP–MS MI analysis is cost and time efficient; hence, it could be performed on a series of assemblages in order to constrain the overall evolution of the igneous system and to identify critical assemblages on which to obtain specific analyses by other techniques.

POTENTIAL INACCURACIES FOR *IN SITU* MICROBEAM DATA

The *analytical accuracy* of MI data obtained from the various techniques has been repeatedly shown elsewhere. Pettke *et al*. (2004) demonstrated that MI data on crystallized and reheated MI acquired with EPMA, SIMS and LA–ICP–MS overlap within their uncertainties (see also Fig. 3-7), and Halter *et al*. (2004a) showed that bulk MI analyzed from coexisting clinopyroxene and plagioclase have identical compositions. These results imply that the signal deconvolution of the mixed inclusion interval is correct and document that crystallized bulk MI can be analyzed accurately by LA–ICP–MS.

Analytical precision for average compositions of MI assemblages is comparable between EPMA, SIMS and LA–ICP–MS, and analytical uncertainties can be as good as a few percent at the 1 standard deviation level. Analyses for individual inclusions are less precise for LA–ICP–MS except for large exposed MI analyzed in single spot mode. Here, SIMS and LA–ICP–MS data are of comparable analytical precision. Carefully acquired data by these microbeam techniques are analytically accurate at these precisions. It is now essential to assess how “geologically correct” such microbeam data are, and to identify potential differences in “correctness” among the various microbeam techniques.

A large non-quantifiable source of uncertainty in microbeam data other than those obtained by bulk MI LA–ICP–MS is the amount of host mineral to be remelted into the inclusion during homogenization in the lab prior to analysis. LA–ICP–MS bulk MI analysis does not require this homogenization step because the correct internal standard (itself the limiting parameter for bulk MI LA–ICP–MS analysis; see below) does account for post-entrapment crystallization of host mineral on to inclusion walls. LA–ICP–MS analysis of unexposed MI should therefore be considered as a check on the correctness of host remelting for the analysis of MI by EPMA and SIMS, by using an element concentration or concentration ratio predicted from independent constraints as the internal standard for LA–ICP–MS data reduction.

The accuracy of LA–ICP–MS data most strongly depends on the quality of the internal standard used for data reduction, irrespective of whether the analysis is done as a spot on exposed MI (*e.g.,* Taylor *et al.* 1997, de Hoog *et al.* 2001, Kamenetsky *et al.* 2002, Danyushevsky *et al.* 2000) or by drilling the entire inclusion out of the host mineral (*e.g.,* Audétat *et al.* 2000, Halter *et al.* 2002a,b, Audétat & Pettke 2003). For cases where MI can be reliably homogenized in the lab, the internal standard element concentration may have been determined by EPMA or SIMS; hence any inaccuracy of the values obtained by EPMA or SIMS (*e.g.,* due to inappropriate host mineral re-melting) translates directly to the LA–ICP–MS data quantification. Inverse modeling may also be used to predict initial melt compositions from analytically accurate microbeam analyses; hence, limitations imposed by the modeling affect the accuracy of all microbeam data equally. The sum of the above uncertainties is probably larger than the mere analytical uncertainty irrespective of which analytical technique was used. The overall uncertainty on average element concentrations of MI assemblages as determined by bulk MI LA–ICP–MS analysis is conservatively estimated to be about 10% for elements enriched in the melt.

The possibility to analyze heterogeneous MI that cannot be homogenized in the lab as required for all the other microbeam techniques renders the LA–ICP–MS bulk MI approach so promising. The fact that diffusive loss of H_2O and H^+ are likely to be the dominant cause for the impossibility of homogenizing some MI in the lab at entrapment temperatures renders it possible that many trace element concentrations in such MI have remained essentially unmodified by diffusive processes. This circumstance alludes to the potential of the new technique of LA–ICP–MS bulk MI analysis. Data may now be obtained from MI hitherto inaccessible by microbeam techniques, allowing the study of additional types of MI that are commonly abundant in hydrous magmatic systems ubiquitous in subduction zone settings. It is foreseen that such new data will provide novel constraints on sources and processes in the genesis of hydrous magmas in diverse geotectonic settings.

PROSPECTS FOR CONSTRAINING SUBDUCTION ZONE MAGMATISM

The final part of this chapter tries to illustrate the potential applications of bulk MI analysis by LA–ICP–MS to constrain deep magma processes in subduction zones. To date, it is not possible to review a comprehensive set of results, simply because applications using the LA–ICP–MS bulk inclusion technique in these environments are only emerging. The unique value of LA–ICP–MS bulk inclusion analysis for investigating the chemical composition of shallow, fluid-saturated melts has been demonstrated. Table 3-1 provides a collection of contributions published so far, demonstrating that the research emphasis was on element distribution between co-existing phases in shallow volcano-plutonic complexes and shallow granites (silicate melts and aqueous fluids, including brine and vapor, and halide melts), and to constrain the mobility and enrichment processes of ore-forming metals. First attempts to constrain experimentally the metal distribution between coexisting melt and fluid phases at the magmatic-hydrothermal interface using the bulk inclusion approach (*e.g.*, Simon *et al.* 2005, Hanley *et al.* 2005a) have demonstrated significant mobility of Au and Pt in variably salty fluids.

The Farallón Negro volcano-plutonic complex in Argentina is the only published example where the chemical evolution of the shallow level magma chamber has been reconstructed by using LA–ICP–MS bulk MI data. The comprehensive data set demonstrates, *inter alia*, that the magma formed by mixing of basaltic magma into resident dacitic magma, and that the mixed magma lost its Cu almost quantitatively to an exsolving aqueous fluid phase, which formed the world class Bajo de la Alumbrera porphyry Cu±Au deposit (Halter *et al.* 2002a,b: 2004b, 2005). So far, there have been only sparse first efforts towards constraining deeper processes including melt–melt element partitioning in deeper magma chambers (Kamenetsky 2006; Halter & Heinrich 2006).

Igneous rocks above subduction zones provide compelling chemical evidence that slab components ascend into the hot zone of the mantle wedge and induce partial melting (*e.g.*, Ulmer 2001). During buoyancy-driven ascent, these magmas react with various sources, including the lower arc crust, and magma mixing has been identified as an important process in the formation of andesitic magmas. These magmas may reside in shallow interconnected reservoirs, evolve and feed volcano-plutonic centers, some of which host the largest magmatic-hydrothermal Cu–Mo–Au ore deposits (*e.g.*, Bingham and Pinatubo: Hattori & Keith 2001; the central Andes: Kay & Mpodozis 2001).

The thorough chemical characterization of the resultant magmatic rocks was used in various ways to extrapolate towards the processes that formed them and to constrain the nature of source components from the arc crust, the mantle wedge and the subducted slab (*e.g.*, Perfit *et al.* 1980, Tatsumi 1989, Morris *et al.* 1990, McGulloch & Gamble 1991, Hawkesworth *et al.* 1993, Plank & Langmuir 1993, and many subsequent publications). Most of the data are from lavas that underwent shallow level fractionation, crystallization, magma mixing and degassing. Original magma characteristics are blurred by these shallow level processes, however. It is thus not surprising that the various source components and their relative importance for the generation of arc magmas have been hotly debated for more than two decades, and

TABLE 3-1: TECHNIQUES DEVELOPMENT AND APPLICATIONS OF THE BULK MI ANALYSIS BY LA-ICP-MS

Development	**Application**	**Comments**	**Reference**
First quantitative analysis of entire crystallized silicate MI	Fluid–melt element distribution at magmatic-hydrothermal stage	Quantification using EPMA data of homogenized MI	Audétat *et al.* 2000
First analysis of entire silicate MI in LA–ICP–MS DRC mode	Improvement in LOD for Ca and Fe using Dynamic Reaction Cell (DRC) technology	Constant Al concentration from EPMA used for quantification	Günther *et al.* 2001
General case of mathematical signal quantification strategy for entire MI	Chemical quantification of entire MI drilled out of host minerals of any chemical composition	Individual MI compositional data with associated analytical uncertainties	Halter *et al.* 2002a
First quantitative analysis of entire sulfide MI	Estimation of Cu/Au ratios in source magma of porphyry-type ore deposits	Calibration of sulfide MI using silicate glass SRM610 from NIST	Halter *et al.* 2002b
Data for highly fractionated MI from barren intrusions	Fluid – melt element distribution in highly fractionated miarolitic cavities	Mg/Al concentration ratio used to quantify MI	Audétat & Pettke, 2003
Demonstration of accuracy of bulk LA–ICP–MS MI analysis	Data comparison between bulk MI (crystallized or reheated) by LA–ICP–MS, and spot analysis by EPMA and SIMS	Evaluation of potential inaccuracies in bulk MI LA–ICP–MS data sets	Pettke *et al.* 2004
Demonstration of accuracy of bulk LA–ICP–MS MI analysis	MI data from co-existing plagioclase and pyroxene identical	Accurate LA–ICP–MS sulfide Fe, Co, Ni, Cu data by standardization on SRM610 from NIST	Halter *et al.* 2004a
First comprehensive study of the life-time evolution of a supra-subduction zone magmatic complex	Quantify chemical characteristics of magma of the ore-forming Farallón Negro Volcano-Plutonic complex	Magma mixing, not evident from bulk-rock data, demonstrated using MI analyses	Halter *et al.* 2004b
Analysis of heterogeneous melt and mineral inclusions	Constrain magma characteristics prior to porphyry-type ore formation	Combined with EPMA and Raman data to constrain S speciation and f_{O2}	Audétat *et al.* 2004
Cu–Au distribution between co-existing sulfide and silicate MI	Constrain source magma processes relevant for porphyry-type ore formation	Identification of sinks for Cu and Au in andesitic magma	Halter *et al.* 2005
Chemical characterization of halide MI	Constraining the genesis of PGE mineralization in quartz veins of the Sudbury Igneous complex	Halide melts distinguished from halite inclusions by trace element inventories	Hanley *et al.* 2005b

that geochemical arguments appeared to be sometimes at odds with geophysical constraints.

Only recently, the value of MI to explore characteristics of deep subduction zone magmas has become broadly appreciated (*e.g.,* Lowenstern 1995, Sobolev 1996, Kamenetsky *et al.* 1997, de Hoog *et al.* 2001, Grove *et al.* 2002, Schiano *et al.* 2004a, Wallace 2005), notably because it could be demonstrated that MI preserve more closely the volatile budget of melts present early in the evolution of eruptive rocks. In other words, the MI represent a more pristine sample than the bulk rock provides. Accordingly, MI trapped in early crystallized minerals better approach pristine samples of mantle-derived melts before shallow level processes disturb their characteristics. This increasing acceptance of MI data currently stimulates research efforts including urgently needed investigations on how MI form in mantle minerals (*e.g.,* Faure & Schiano 2005) and on the fundamental issues of post-entrapment modifications of bulk MI compositions. Such data are prerequisite for the proper application of MI to the study of subduction zone processes in particular, because here, the mobile phase(s) is (are) a driving force in this dynamic environment.

Water contents as high as 10 wt.% in MI from high-Mg andesites have been reported (*e.g.,* Anderson 1974, Sisson & Layne 1993, Grove *et al.* 2002, Straub & Layne 2003). Such high water contents are not known from island arc rocks, revealing that these magmas degas significantly before solidification or eruption. A strong link between water and elements typically enriched in subduction zone magmas such as large ion lithophile elements (LILE) and light rare earth elements (LREE; *e.g.,* Sobolev & Danyushevsky 1994, Stolper & Newman 1994, Grove *et al.* 2002, Cervantes & Wallace 2003) demonstrate that these elements are enriched in the mobile phase ascending from the slab. This hypothesis has been corroborated by experiment (*e.g.,* Brenan *et al.* 1995, Keppler 1996, Johnson & Plank 1999), most recently for basalt equilibrated with water at pressures of 4–6 GPa, corresponding to slab depth encountered beneath arcs (Kessel *et al.* 2005a,b). This mobile component, irrespective of whether it is an aqueous fluid or a hydrous melt, or a supercritical liquid beyond the second critical end point at 5–6 GPa, produced a multiphase quench product trapped in a diamond trap. This diamond trap in the experimental capsule resembles "a very large MI" that can be quantitatively analyzed at ambient pressure conditions only by cryogenic LA–ICP–MS (Kessel *et al.* 2004). The various mobile components are relatively enriched in LILE and LREE, and element concentrations generally increase with increasing pressure. Supercritical liquids are essentially identical in trace element signatures with hydrous melts existing at lower pressure (Kessel *et al.* 2005a), implying that "established" trace element fingerprints for slab melting are no longer unique in their interpretation. Such "slab melt signatures" may thus indicate that the slab component corresponds to a supercritical liquid of potentially highly variable water contents, notably in mature and fast subduction zone settings. This also signifies relaxing of the apparent temperature discrepancy between geochemical arguments and geophysical models for the temperature regimes in slabs beneath island arcs (Kessel *et al.* 2005a).

MI provide the most promising approach to explore further the least modified slab component interpreted to be inherently water-rich and present in "undegassed" magma, allowing a test of how generally applicable these experimental data obtained on a Cl- and S-free system (Kessel *et al.* 2005a,b) are in nature. Notably the effect of chlorinity may be profound in shifting some of these slab element signatures, and there is evidence for highly variable chlorinity in slab components (*e.g.,* Kent *et al.* 2002; summarized in Wallace 2005). MI having trapped such undegassed magma will also provide the closest approach to pristine concentrations of mobile trace elements in general, *e.g.,* Li, B, Cu, Pb or halogens to name only a few. The mere occurrence of some of these elements in volcanic exhalatives (*e.g.,* Nho *et al.* 1996) suggests that their primary abundance in degassed magma may be severely reduced. Consequently, MI trapped early in magma genesis at subduction zones may represent, most closely, the fertile component that renders subduction zone magmas so distinct; hence, it is these MI that constrain the slab input to the magma most reliably. But it is exactly these MI that are most prone to diffusive loss of volatiles during prolonged residence at depth, notably water, rendering their proper homogenization impossible – if recognized as inclusions in primitive samples, *e.g.,* in forsterite-rich olivine, LA–ICP–MS is currently the only tool to constrain their chemical composition including most of the mobile elements. Careful geological interpretation of such data will significantly advance our understanding of the slab contribution to magma formation at convergent margins.

Another window on chemical characteristics of deep subduction zone magmas is provided by MI from xenoliths or exposed root zones of volcano-plutonic systems including cumulate rocks. Here, MI homogenization is generally difficult because of the extended residence time of such samples at high temperature and pressure conditions, enhancing diffusive equilibration. The investigation of MI in such samples (*e.g.,* Cortini *et al.* 1985, Debari & Sleep 1991, Schiano *et al.* 1995, De Vivo *et al.* 1995, Frezzotti 2001, Spandler *et al.* 2003, Schiano *et al.* 2004b) has already provided fundamental constraints on igneous processes in subduction zones. LA–ICP–MS analyses of heterogeneous inclusions will provide novel chemical data on these deep systems, and the comparison with MI data obtained on Fo-rich olivine from mafic lavas will be most interesting.

Accepting the difficulty of deriving a reliable internal standard for MI quantification, LA–ICP–MS data will nevertheless provide unprecedented information on such (originally) volatile-rich MI, notably for MI trapped in olivine or orthopyroxene. Here, the host mineral is chemically "simple", because most trace elements of interest are present at very low concentrations only. Therefore, removing inappropriate amounts of host mineral from the mixed inclusion signal interval will change the abundances of such trace elements in the MI by the same factor, *i.e.*, the *trace element ratios* and, thus, *normalized trace element patterns* (*e.g.*, REE spectra, spider diagrams) of the MI will remain the same. Such high precision trace element signatures do not require internal standardization at all, they are uniquely defined by the use of external standardization only in LA–ICP–MS analysis. Many supra-subduction igneous processes are constrained by using element abundance ratios alone, *e.g.*, Sr/Y, U/Th, Ba/La or B/Be, or isotopic ratios such as ^{10}Be/^{11}Be (*e.g.*, Morris *et al.* 1990, McCulloch & Gamble 1991, Plank & Langmuir 1993, Hawkesworth *et al.* 1993, Johnson & Plank 1999), and bulk MI LA–ICP–MS will significantly increase this data set on hydrous igneous systems.

Evidently, LA–ICP–MS bulk MI data from inclusions that cannot be homogenized reliably in the lab hold great potential for further constraining the signature of the (originally) most volatile-rich components in subduction zone magma systems, thus potentially shrinking the "black box" between what is liberated from the slab as known from high pressure experiments and what can be sampled in primitive arc magma end members.

ACKNOWLEDGEMENTS

My experience in the analysis of MI by LA–ICP–MS has greatly benefited from the various research projects in the group of Chris Heinrich at ETH Zurich, notably from the close collaboration with Werner Halter, and from collaborative work with Andreas Audétat, Adam Simon and Jacob Hanley. I am very grateful for the thoughtful reviews by Terry Plank and Leonid Danyushevsky, and the great editorial help by Jim Webster, substantially improving the present contribution. Constructive suggestions on an early version of this manuscript by O. Müntener and János Kodolányi are appreciated. I gratefully acknowledge funding from the Swiss National Science Foundation.

REFERENCES

AESCHLIMAN, D.B., BAJIC, S.J., BALDWIN, D.P. & HOUK, R.S. (2003): High-speed digital photographic study of an inductively coupled plasma during laser ablation: comparison of dried solution aerosols from a microconcentric nebulizer and solid particles from laser ablation. *J. Anal. Atom. Spectrom.* **18**(9), 1008–1014.

ANDERSON, A.T. (1974): Evidence for a picritic, volatile-rich magma beneath Mt Shasta, California. *J. Petrol.* **15**(2), 243–267.

AUDÉTAT, A. & PETTKE, T. (2003): The magmatic-hydrothermal evolution of two barren granites: A melt and fluid inclusion study of the Rito del Medio and Canada Pinabete plutons in northern New Mexico (USA). *Geochmim. Cosmochim. Acta* **67**(1), 97–121.

AUDÉTAT, A., PETTKE, T. & DOLEJS, D. (2004): Magmatic anhydrite and calcite in the ore-forming quartz- monzodiorite magma at Santa Rita, New Mexico (USA): genetic constraints on porphyry-Cu mineralization. *Lithos* **72**(3–4), 147–161.

AUDÉTAT, A., GÜNTHER, D. & HEINRICH, C.A. (2000): Magmatic-hydrothermal evolution in a fractionating granite: A microchemical study of the Sn–W–F-mineralized Mole Granite (Australia). *Geochmim. Cosmochim. Acta* **64**(19), 3373–3393.

BODNAR, R.J. & STUDENT, J.J. (2006): Melt inclusions in plutonic rocks: petrography and microthermometry. *In* Melt Inclusions in Plutonic Rocks (J.D. Webster, *ed.*) Min. Assoc. Can. Short Course **36**, 1-25.

BOGAERTS, A. & CHEN, Z.Y. (2005): Effect of laser parameters on laser ablation and laser-induced plasma formation: A numerical modelling investigation. *Spectrochim. Acta Part B–At. Spectrosc.* **60**(9–10), 1280–1307.

BORISOV, O.V., MAO, X.L. & RUSSO, R.E. (2000): Effects of crater development on fractionation and signal intensity during laser ablation inductively coupled plasma mass spectrometry. *Spectrochim. Acta Part B–At. Spectrosc.* **55**(11), 1693–1704.

BRENAN, J.M., SHAW, H.F., RYERSON, F.J. & PHINNEY, D.L. (1995): Mineral-aqueous fluid partitioning of trace elements at 900 degrees C and 2.0 GPa: Constraints on the trace element chemistry of mantle and deep crustal fluids. *Geochim. Cosmochim. Acta* **59**(16), 3331–3350.

CERVANTES, P. & WALLACE, P.J. (2003): Role of H_2O in subduction-zone magmatism: New insights from melt inclusions in high-Mg basalts from central Mexico. *Geology* **31**(3), 235–238.

CLOCCHIATTI, R. (1977): Melt inclusions in olivine, plagioclase and pyroxene phenocrystals as samples of magmatic liquid during host mineral crystallization – application to a low K basalt of emerged mid-oceanic ridge (Asal, Tfai). *Comptes Rendus Hebdomadaires Des Seances De L' Academie Des Sciences Serie D* **284**(22), 2203.

CORTINI, M., LIMA, A. & DE VIVO, B. (1985): Trapping temperatures of melt inclusions from ejected Vesuvian mafic xenoliths. *J. Volcanol. Geotherm. Res.* **26**(1–2), 167–172.

COTTRELL, E., SPIEGELMAN, M. & LANGMUIR, C.H. (2002): Consequences of diffusive reequilibration for the interpretation of melt inclusions. *Geochem. Geophys. Geosys.* **3**, art. no. 1026.

DANYUSHEVSKY, L.V., DELLA-PASQUA, F.N. & SOKOLOV, S. (2000): Re-equilibration of melt inclusions trapped by magnesian olivine phenocrysts from subduction-related magmas: petrological implications. *Contrib. Min. Petrol.* **138**(1), 68–83.

DANYUSHEVSKY, L.V., LESLIE, R.A.J., CRAWFORD, A.J. & DURANCE, P. (2004): Melt inclusions in primitive olivine phenocrysts: The role of localized reaction processes in the origin of anomalous compositions. *J. Petrol.* **45**(12), 2531–2553.

DANYUSHEVSKY, L.V., MCNEILL, A.W. & SOBOLEV, A.V. (2002): Experimental and petrological studies of melt inclusions in phenocrysts from mantle-derived magmas: an overview of techniques, advantages and complications. *Chem. Geol.* **183**(1–4), 5–24.

DEBARI, S.M. & SLEEP, N.H. (1991): High-Mg, low-Al bulk composition of the Talkeetna Island Arc, Alaska – implications for primary magmas and the nature of arc crust. *Geol. Soc. Amer. Bull.* **103**(1), 37–47.

DE HOOG, J.C.M., MASON, P.R.D. & VAN BERGEN, M.J. (2001): Sulfur and chalcophile elements in subduction zones: Constraints from a laser ablation ICP–MS study of melt inclusions from Galunggung Volcano, Indonesia. *Geochmim. Cosmochim. Acta* **65**(18), 3147–3164.

DE VIVO, B., TOROK, K., AYUSO, R.A., LIMA, A. & LIRER, L. (1995): Fluid inclusion evidence for magmatic silicate/saline/CO_2 immiscibility and geochemistry of alkaline xenoliths from Ventotene Island, Italy. *Geochmim. Cosmochim. Acta* **59**(14), 2941–2953.

EGGINS, S., DE DECKKER, P. & MARSHALL, J. (2003): Mg/Ca variation in planktonic foraminafera tests: implications for reconstructing palaeoseawater temperature and habitat migration. *Earth Planet. Sci. Lett.* **212**(3–4), 291–306.

EGGINS, S., KINSLEY, L.P.J. & SHELLEY, J.M.G. (1998): Deposition and element fractionation processes during atmospheric pressure laser sampling for analysis by ICP–MS. *Appl. Surf. Sci.* **129**, 278–286.

EVANS P., WOLFF-BRICHE, C. & FAIRMAN, B. (2001): High accuracy analysis of low level sulfur in diesel fuel by isotope dilution high resolution ICP–MS, using silicon for mass bias correction of natural isotope ratios. *J. Anal. Atom. Spectrom.* **16**(9), 964–969.

FAURE F. & SCHIANO P. (2005): Experimental investigation of equilibration conditions during forsterite growth and melt inclusion formation. *Earth Planet. Sci. Lett.* **236**(3–4), 882–898.

FREZZOTTI M.L. (2001): Silicate-melt inclusions in magmatic rocks: applications to petrology. *Lithos* **55**(1–4), 273–299.

FRYER, B.J., JACKSON, S.E. & LONGERICH, H.P. (1995): Design, operation and role of the laser-ablation microprobe coupled with an inductively coupled plasma mass spectrometer (LAM–ICP–MS) in the earth sciences. *Can. Mineral.* **33**, 303–312.

GAETANI, G.A. & WATSON, E.B. (2000): Open system behavior of olivine-hosted melt inclusions. *Earth Planet. Sci. Lett.* **183**(1–2), 27–41.

GOLDSTEIN, J.L., NEWBURY, D.E., ECHLIN, P., JOY, D.C., ROMIG, A.D., LYMAN, C.E., FIORI, C. & LIFSHIN, E. (1992): Scanning electron microscopy and X-ray microanalysis. 2nd edition. Plenum Press, New York, 820p.

GRAY, A.L. (1985): Solid sample introduction by laser ablation for inductively coupled plasma source–mass spectrometry. *Analyst* **110**(5), 551–556.

GROVE, T.L., PARMAN, S.W., BOWRING, S.A., PRICE, R.C. & BAKER, M.B. (2002): The role of an H_2O-rich fluid component in the generation of primitive basaltic andesites and andesites from the Mt. Shasta region, N California. *Contrib. Min. Petrol.* **142**(4), 375–396.

GUILLONG, M. & GÜNTHER, D. (2002): Effect of particle size distribution on ICP-induced elemental fractionation in laser ablation–inductively coupled plasma–mass spectrometry. *J. Anal. Atom. Spectrom.* **17**(8), 831–837.

GUILLONG, M., HORN, I. & GÜNTHER, D. (2003a): A comparison of 266 nm, 213 nm and 193 nm produced from a single solid state Nd : YAG laser for laser ablation ICP–MS. *J. Anal. Atom. Spectrom.* **18**(10), 1224–1230.

GUILLONG M., KUHN H.R. & GÜNTHER D. (2003b): Application of a particle separation device to reduce inductively coupled plasma-enhanced elemental fractionation in laser ablation–inductively coupled plasma–mass spectrometry. *Spectrochim. Acta Part B–At. Spectrosc.* **58**(2–3), 211–220.

GÜNTHER, D., AUDÉTAT, A., FRISCHKNECHT, R. & HEINRICH C.A. (1998): Quantitative analysis of major, minor and trace elements in fluid inclusions using laser ablation inductively coupled plasma mass spectrometry. *J. Anal. Atom. Spectrom.* **13**(4), 263-270.

GÜNTHER D. & HATTENDORF, B. (2005): Solid sample analysis using laser ablation inductively coupled plasma mass spectrometry. *Trac-Trends in Anal. Chem.* **24**(3), 255–265.

GÜNTHER, D., HATTENDORF, B. & AUDÉTAT, A. (2001): Multi-element analysis of melt and fluid inclusions with improved detection capabilities for Ca and Fe using laser ablation with a dynamic reaction cell ICP–MS. *J. Anal. Atom. Spectrom.* **16**(9), 1085–1090.

GÜNTHER, D., FRISCHKNECHT, R., HEINRICH, C.A. & KAHLERT, H.J. (1997): Capabilities of an Argon Fluoride 193 nm excimer laser for laser ablation inductively coupled plasma mass spectrometry microanalysis of geological materials. *J. Anal. Atom. Spectrom.* **12**(9), 939–944.

HALTER, W.E. & HEINRICH, C.A. (2005): Magmatic processes and volatile phase generation in porphyry-type environments: A laser ablation–ICP–MS study of silicate and sulfide melt inclusions. *In* Melt Inclusions in Plutonic Rocks (J.D. Webster, *ed.*) Min. Assoc. Can. Short Course **36**, 151-164.

HALTER W., HEINRICH C.A. & PETTKE T. (2005): Magma evolution and the formation of porphyry Cu–Au ore fluids: evidence from silicate and sulfide melt inclusions. *Mineral. Dep.* **39**(8), 845–863.

HALTER, W., HEINRICH, C.A. & PETTKE, T. (2004b): Laser–ablation ICP–MS analysis of silicate and sulfide melt inclusions in an andesitic complex II: evidence for magma mixing and magma chamber evolution. *Contrib. Min. Petrol.* **147**(4), 397–412.

HALTER, W., PETTKE ,T. & HEINRICH, C.A. (2002b): The origin of Cu/Au ratios in porphyry-type ore deposits. *Science* **296**(5574), 1844–1846.

HALTER, W., PETTKE, T. & HEINRICH, C.A. (2004a): Laser–ablation ICP–MS analysis of silicate and sulfide melt inclusions in an andesitic complex I: analytical approach and data evaluation. *Contrib. Min. Petrol.* **147**(4), 385–396.

HALTER, W., PETTKE, T. & HEINRICH, C.A. & ROTHEN-RUTISHAUSER, B. (2002a): Major to trace element analysis of melt inclusions by laser-ablation ICP–MS: methods of quantification. *Chem. Geol.* **183**(1–4), 63–86.

HANLEY, J.J., PETTKE, T., MUNGALL, J.E. & SPOONER, E.T.C. (2005a): The solubility of platinum and gold in NaCl brines at 1.5 kbar, 600 to 800 degrees C: A laser ablation ICP–MS pilot study of synthetic fluid inclusions. *Geochmim. Cosmochim. Acta* **69**(10), 2593–2611.

HANLEY, J.J., MUNGALL, J.E., PETTKE, T., SPOONER, E.T.C. & BRAY, C.J. (2005b): Ore metal redistribution by hydrocarbon–brine and hydrocarbon–halide melt phases, North Range footwall of the Sudbury Igneous Complex, Ontario, Canada. *Mineral. Dep.* **40**(3), 237–256.

HATTENDORF, B. & GÜNTHER, D. (2000): Characteristics and capabilities of an ICP–MS with a dynamic reaction cell for dry aerosols and laser ablation. *J. Anal. Atom. Spectrom.* **15**(9), 1125–1131.

HATTORI, K.H. & KEITH, J.D. (2001): Contribution of mafic melt to porphyry copper mineralization: evidence from Mount Pinatubo, Philippines, and Bingham Canyon, Utah, USA. *Mineral. Dep.* **36**(8), 799–806.

HAURI, E., WANG, J.H., DIXON, J.E., KING, P.L., MANDEVILLE, C. & NEWMAN, S. (2002): SIMS analysis of volatiles in silicate glasses 1. Calibration, matrix effects and comparisons with FTIR. *Chem. Geol.* **183**(1–4), 99–114.

HAWKESWORTH, C.J., GALLAGHER, K., HERGT, J.M. & MCDERMOTT, F. (1993): Trace-element fractionation processes in the generation of island-arc basalts. *Philosophical Transactions of the Royal Society of London Series A – Mathematical Physical and Engineering Sciences* **342**(1663), 179–191.

HEINRICH, C.A., PETTKE, T., HALTER, W.E., AIGNER-TORRES, M., AUDÉTAT, A., GÜNTHER, D., HATTENDORF, B., BLEINER, D., GUILLONG, M. & HORN, I. (2003): Quantitative multi-element analysis of minerals, fluid and melt inclusions by laser-ablation inductively-coupled-plasma mass-spectrometry. *Geochim. Cosmochim. Acta* **67**(18), 3473–3497.

HELLEBRAND, E., SNOW, J.E., MOSTEFAOUI, S. & HOPPE P. (2005): Trace element distribution between orthopyroxene and clinopyroxene in peridotites from the Gakkel Ridge: a SIMS and NanoSIMS study. *Contrib. Min. Pet.* **150**(5), 486–504.

HORN, I., GUILLONG, M. & GÜNTHER, D. (2001): Wavelength dependant ablation rates for metals and silicate glasses using homogenized laser beam profiles – implications for LA–ICP–MS. *Appl. Surf. Sci.* **182**(1–2), 91–102.

IHINGER, P.D., HERVIG, R.L. & MCMILLAN, P.F. (1994): Analytical methods for volatiles in magmas. In: Carrol, M.R. and Holloway, J.R. (eds), *Rev. Mineral.* **30**, 67–129

JACKSON, S.E. & GÜNTHER, D. (2003): The nature and sources of laser induced isotopic fractionation in laser ablation–multicollector-inductively coupled plasma– mass spectrometry. *J. Anal. Atom. Spectrom.* **18**(3), 205–212.

JACKSON, S.E., LONGERICH, H.P., DUNNING, G.R. & FRYER, B.J. (1992): The application of laser-ablation microprobe–inductively coupled plasma–mass-spectrometry (LAM–ICP–MS) to *in situ* trace-element determinations in minerals. *Can. Mineral.* **30**, 1049–1064.

JEFFRIES, T.E., PEARCE, N.J.G., PERKINS, W.T. & RAITH, A. (1996): Chemical fractionation during infrared and ultraviolet laser ablation inductively coupled plasma mass spectrometry – Implications for mineral microanalysis. *Analyt. Commun.* **33**(1), 35–39.

JENNER, G.A., FOLEY, S.F., JACKSON, S.E., GREEN, T.H., FRYER, B.J. & LONGERICH, H.P. (1993): Determination of partition coefficients for trace elements in high pressure temperature experimental run products by laser ablation microprobe–inductively coupled plasma–mass spectrometry (LAM–ICP–MS). *Geochim. Cosmochim. Acta* **57**(23–24), 5099–5103.

JOHNSON, M.-C. & PLANK, T. (1999): Dehydration and melting experiments constrain the fate of subducted sediment. *Geochem. Geophys. Geosys.***1**, doi:10.1029/1999GC000014 1999.

KAMENETSKY, V.S. (2006): Melt inclusion record of magmatic immiscibility in crustal and mantle magmas. *In* Melt Inclusions in Plutonic Rocks (J.D. Webster, *ed.*) Min. Assoc. Can. Short Course **36**, 81-98.

KAMENETSKY, V.S., CRAWFORD, A.J., EGGINS, S. & MUHE, R. (1997): Phenocryst and melt inclusion chemistry of near-axis seamounts, Valu Fa Ridge, Lau Basin: insight into mantle wedge melting and the addition of subduction components. *Earth Planet. Sci. Lett.* **151**(3–4), 205–223.

KAMENETSKY, V.S. & DANYUSHEVSKY, L.V. (2005): Metals in quartz-hosted melt inclusions: Natural facts and experimental artifacts. *Am. Mineral.* **90**(10), 1674–1678.

KAMENETSKY, V.S., SOBOLEV, A.V., EGGINS, S.M., CRAWFORD, A.J. & ARCULUS, R.J. (2002): Olivine-enriched melt inclusions in chromites from low-Ca boninites, Cape Vogel, Papua New Guinea: evidence for ultramafic primary magma, refractory mantle source and enriched components. *Chem. Geol.* **183**(1–4), 287–303.

KAMENETSKY, V.S., WOLFE, R.C., EGGINS, S.M., MERNAGH, T.P. & BASTRAKOV, E. (1999): Volatile exsolution at the Dinkidi Cu–Au porphyry deposit, Philippines: A melt–inclusion record of the initial ore-forming process. *Geology* **27**(8), 691–694.

KAY, S.M & MPODOZIS, C. (2001): Central Andean ore deposits linked to evolving shallow subduction systems and thickened crust. *GSA Today* **11**(3), 4–9.

KENT, A.J.R., PEATE, D.W., NEWMAN, S., STOLPER, E.M. & PEARCE J.A. (2002): Chlorine in submarine glasses from the Lau Basin: seawater contamination and constraints on the composition of slab-derived fluids. *Earth Planet. Sci. Lett.* **202**(2), 361–377.

KEPPLER, H. (1996): Constraints from partitioning experiments on the composition of subduction-zone fluids. *Nature* **380**(6571), 237–240.

KESSEL, R., SCHMIDT, M.W., ULMER, P. & PETTKE, T. (2005a): Trace element signature of subduction-zone fluids, melts and supercritical liquids at 120–180 km depth. *Nature* **437**(7059), 724–727.

KESSEL, R., ULMER, P., PETTKE, T., SCHMIDT, M.W. & THOMPSON, A.B. (2005b): The water–basalt system at 4 to 6 GPa: Phase relations and second critical endpoint in a K-free eclogite at 700 to 1400 degrees C. *Earth Planet. Sci. Lett.* **237**(3–4), 873–892.

KESSEL, R., ULMER, P., PETTKE, T., SCHMIDT, M.W. & THOMPSON, A.B. (2004): A novel approach to determine high-pressure high-temperature fluid and melt compositions using diamond-trap experiments. *Am. Mineral.* **89**(7), 1078–1086.

KRESS, V.C. & GHIORSO, M.S. (2004): Thermodynamic modeling of post-entrapment crystallization in igneous phases. *J. Volcanol. Geotherm. Res.* **137**(4), 247–260.

KUHN, H.R. & GÜNTHER, D. (2004): Laser ablation–ICP–MS: particle size dependent elemental composition studies on filter-collected and online measured aerosols from glass. *J. Anal. Atom. Spectrom.* **19**(9) 1158–1164.

LAHAYE, Y., BENDALL, C., BREY, G., FIEBIG, J. & WEYER S. (2004): *In situ* sulfur isotope ratio measurements by laser ablation high resolution MC–ICP–MS. *Geochim. Cosmochim. Acta* **68**(11), A69–A69.

LATKOCZY, C. & GÜNTHER, D. (2002): Enhanced sensitivity in inductively coupled plasma sector field mass spectrometry for direct solid analysis using laser ablation (LA–ICP–SFMS). *J. Anal. Atom. Spectrom.* **17**(10), 1264–1270.

LAYNE, G.D. (2006): Application of secondary ion mass spectrometry to the determination of traditional and non-traditional light stable isotopes in melt inclusions. *In* Melt Inclusions in Plutonic Rocks (J.D. Webster, *ed.*) Min. Assoc. Can. Short Course **36**, 27-49.

LEACH, A.M. & HIEFTJE, G.M. (2000): Methods for shot-to-shot normalization in laser ablation with an inductively coupled plasma time-of-flight mass spectrometer. *J. Anal. Atom. Spectrom.* **15**(9), 1121–1124.

LONGERICH, H.P., GÜNTHER, D. & JACKSON, S.E. (1996b): Elemental fractionation in laser ablation inductively coupled plasma mass spectrometry. *Fresen. J. Anal. Chem.* **355**(5–6), 538–542.

LONGERICH H.P., JACKSON, S.E. & GÜNTHER, D. (1996a): Laser ablation inductively coupled plasma mass spectrometric transient signal data acquisition and analyte concentration calculation. *J. Anal. Atom. Spectrom.* **11**(9), 899–904.

LOWENSTERN, J.B. (1995): Applications of silicate–melt inclusions to the study of magmatic volatiles. In *MAC, Short Course Series* **23** (ed. F.H. Thompson), pp. 71–99.

LOWENSTERN, J.B. & MAHOOD, G.A. (1991): New data on magmatic H_2O contents of pantellerites, with implications for petrogenesis and eruptive dynamics at Pantelleria. *Bull. Volcanol.* **54**(1), 78–83.

LUDWIG, K.R. (1994): ISOPLOT: A plotting and regression program for radiogenic isotope data, for IBM–PC compatible computers, version 2.71. *USGS Open file Report* **91–445**.

LUHR, J.F. (2001): Glass inclusions and melt volatile contents at Paricutin Volcano, Mexico. *Contrib. Min. Petrol.* **142**(3), 261–283.

MCCULLOCH, M.T. & GAMBLE, J.A. (1991): Geochemical and geodynamical constraints on subduction zone magmatism. *Earth Planet. Sci. Lett.* **102**(3–4), 358–374.

METRICH, N. & CLOCCHIATTI, R. (1989): Melt inclusion investigation of the volatile behavior in historic alkali basalt magmas of Etna. *Bull. Volcanol.* **51**(3), 185-198.

METRICH, N. & CLOCCHIATTI, R. (1996): Sulfur abundance and its speciation in oxidized alkaline melts. *Geochmim. Cosmochim. Acta* **60**(21), 4151–4160.

MORRIS, J.D., LEEMAN, W.P. & TERA, F. (1990): The subducted component in island arc lavas – constraints from Be isotopes and B–Be systematics. *Nature* **344**(6261), 31–36.

NEWMAN, S., STOLPER, E.M. & EPSTEIN, S. (1986): Measurement of water in rhyolitic glasses – calibration of an infrared spectroscopic technique. *Am. Mineral.* **71**(11–12), 1527–1541.

NHO, E.Y., LECLOAREC, M.F., ARDOUIN, B. & TJETJEP, W.S. (1996): Source strength assessment of volcanic trace elements emitted from the Indonesian arc. *J. Volcanol. Geotherm. Res.* **74**(1–2), 121–129.

PERFIT, M.R., GUST, D.A., BENCE, A.E., ARCULUS, R.J. & TAYLOR, S.R. (1980): Chemical characteristics of island arc basalts – implications for mantle sources. *Chem. Geol.* **30**(3), 227–256.

PETTKE, T., HEINRICH, C.A., CIOCAN, A.C. & GÜNTHER, D. (2000): Quadrupole mass spectrometry and optical emission spectroscopy: detection capabilities and representative sampling of short transient signals from laser ablation. *J. Anal. Atom. Spectrom.* **15**(9), 1149–1155.

PETTKE, T., HALTER, W.E., WEBSTER, J.D., AIGNER-TORRES, M. & HEINRICH, C.A. (2004): Accurate quantification of melt inclusion chem.-istry by LA–ICP–MS: a comparison with EMP and SIMS and advantages and possible limitations of these methods. *Lithos* **78**(4), 333–361.

PLANK, T. & LANGMUIR, C.H. (1993): Tracing trace elements from sediment input to volcanic output at subduction zones. *Nature* **362**(6422), 739–743.

POITRASSON, F., MAO, X.L., MAO, S.S., FREYDIER, R. & RUSSO, R.E. (2003): Comparison of ultraviolet femtosecond and nanosecond laser ablation inductively coupled plasma mass spectrometry analysis in glass, monazite, and zircon. *Anal. Chem.* **75**(22), 6184–6190.

QIN, Z.W., LU, F.Q. & ANDERSON, A.T. (1992): Diffusive reequilibration of melt and fluid inclusions. *Am. Mineral.* **77**(5–6), 565–576.

RAMSEY, M.H., COLES, B. J., WILKINSON, J.J., & RANKIN, A.H. (1992): Single fluid inclusion analysis by laser ablation inductively coupled plasma atomic emission spectrometry – quantification and validation. *J. Anal. Atom. Spectrom.* **7**(4), 587–593.

ROEDDER, E. (1979): Origin and significance of magmatic inclusions. *Bull Minéral.* **102**(5–6), 487–510.

ROEDDER, E. (1984): Fluid Inclusions. *Rev. Mineral.* **12**. Mineralogical Society of America, pp 645.

RUSSO, R.E., MAO, X.L., LIU, C. & GONZALEZ, J. (2004): Laser assisted plasma spectrochemistry: laser ablation. *J. Anal. Atom. Spectrom.* **19**(9), 1084–1089.

SCHIANO, P. (2003): Primitive mantle magmas recorded as silicate melt inclusions in igneous minerals. *Earth Sci. Rev.* **63**(1–2), 121–144.

SCHIANO P., CLOCCHIATTI R., BOIVIN P. & MEDARD E. (2004b): The nature of melt inclusions inside minerals in an ultramafic cumulate from Adak volcanic center, aleutian arc: implications for the origin of high-Al basalts. *Chem. Geol.* **203**(1–2), 169–179.

SCHIANO, P., CLOCCHIATTI, R., OTTOLINI, L. & SBRANA, A. (2004a): The relationship between potassic, calc-alkaline and Na-alkaline magmatism in South Italy volcanoes: A melt inclusion approach. *Earth Planet. Sci. Lett.* **220**(1–2), 121–137.

SCHIANO, P., CLOCCHIATTI, R., SHIMIZU, N., MAURY, R.C., JOCHUM, K.P. & HOFMANN, A.W. (1995): Hydrous, silica-rich melts in the sub-arc mantle and their relationship with erupted arc lavas. *Nature* **377**(6550), 595–600.

SIMON, A.C., FRANK, M.R., PETTKE ,T., CANDELA, P.A., PICCOLI, P.M. & HEINRICH, C.A. (2005): Gold partitioning in melt–vapor–brine systems. *Geochmim. Cosmochim. Acta* **69**(13), 3321–3335.

SISSON, T.W. & LAYNE, G.D. (1993): H_2O in basalt and basaltic andesite glass inclusions from 4 subduction-related volcanos. *Earth Planet. Sci. Lett.* **117**(3–4), 619–635.

SOBOLEV, A.V. (1996): Melt inclusions in minerals as a source of principle petrological information. *Petrology* **4**(3), 209–220.

SOBOLEV, A.V. & CHAUSSIDON, M. (1996): H_2O concentrations in primary melts from supra-subduction zones and mid-ocean ridges: Implications for H_2O storage and recycling in the mantle. *Earth Planet. Sci. Lett.* **137**(1–4), 45–55.

SOBOLEV, A.V. & DANYUSHEVSKY, L.V. (1994): Petrology and geochemistry of boninites from the north termination of the Tonga Trench – constraints on the generation conditions of primary high-Ca boninite magmas. *J. Petrol.* **35**(5), 1183–1211.

SPANDLER, C.J., ARCULUS, R.J., EGGINS, S.M., MAVROGENES, J.A., PRICE, R.C. & REAY, A.J. (2003): Petrogenesis of the Greenhills Complex, Southland, New Zealand: magmatic differentiation and cumulate formation at the roots of a Permian island-arc volcano. *Contrib. Min. Petrol.* **144**(6), 703–721.

STADERMANN, F.J., CROAT, T.K., BERNATOWICZ, T.J., AMARI, S., MESSENGER, S., WALKER, R.M. & ZINNER, E. (2005): Supernova graphite in the NanoSIMS: Carbon, oxygen and titanium isotopic compositions of a spherule and its TiC sub-components. *Geochmim. Cosmochim. Acta* **69**(1), 177–188.

STOLPER, E. (1982): Water in silicate glasses – an infrared spectroscopic study. *Contrib. Min. Petrol.* **81**(1) 1–17.

STOLPER, E. & NEWMAN, S. (1994): The role of water in the petrogenesis of Mariana Trough magmas. *Earth Planet. Sci. Lett.* **121**(3–4), 293–325.

STRAUB, S.M. & LAYNE, G.D. (2003): The systematics of chlorine, fluorine, and water in Izu arc front volcanic rocks: Implications for volatile recycling in subduction zones. *Geochmim. Cosmochim. Acta* **67**(21), 4179–4203.

STUDENT, J.J. & BODNAR, R.J. (2004): Silicate melt inclusions in porphyry copper deposits: Identification and homogenization behavior. *Can. Mineral.* **42**, 1583–1599.

TAIT, S. (1992): Selective preservation of melt inclusions in igneous phenocrysts. *Am. Mineral.* **77**(1–2), 146–155.

TATSUMI, Y. (1989): Migration of fluid phases and genesis of basalt magmas in subduction zones. *J: Geophys. Res. – Solid Earth* **94**(B4), 4697–4707.

TAYLOR, R.P., JACKSON, S.E., LONGERICH, H.P. & WEBSTER, J.D. (1997): *In situ* trace element analysis of individual silicate melt inclusions by laser ablation microprobe inductively coupled plasma–mass spectrometry (LAM–ICP–MS). *Geochmim. Cosmochim. Acta* **61**(13), 2559–2567.

THOMAS, R. (2000): Determination of water contents of granite melt inclusions by confocal laser Raman microprobe spectroscopy. *Am. Mineral.* **85**(5–6), 868–872.

ULMER, P. (2001): Partial melting in the mantle wedge – the role of H_2O in the genesis of mantle-derived 'arc-related' magmas. *Physics of the Earth and Planetary Interiors* **127**(1–4), 215–232.

WALLACE, P.J. (2005): Volatiles in subduction zone magmas: concentrations and fluxes based on melt inclusion and volcanic gas data. *J. Volcanol. Geotherm. Res.* **140**(1–3), 217–240.

WALLACE, P.J., ANDERSON, A.T. & DAVIS, A.M. (1999): Gradients in H_2O, CO_2, and exsolved gas in a large volume silicic magma system: Interpreting the record preserved in melt inclusions from the Bishop Tuff. *J: Geophys. Res. – Solid Earth* **104**(B9), 20097–20122.

WATSON, E.B. (1976): Glass inclusions as samples of early magmatic liquid – determinative method and application to a South-Atlantic basalt. *J. Volcanol. Geotherm. Res.* **1**(1), 73–84.

WEBSTER, J.D., THOMAS, R., RHEDE, D., FORSTER, H.J. & SELTMANN, R. (1997): Melt inclusions in quartz from an evolved peraluminous pegmatite: Geochemical evidence for strong tin enrichment in fluorine-rich and phosphorus-rich residual liquids. *Geochmim. Cosmochim. Acta* **61**(13), 2589–2604.

ZAJACZ, Z., HALTER, W.E., MALFAIT, W.J., BACHMANN, O., BODNAR, R.J., HIRSCHMANN, M.M., MANDEVILLE, C.W., MORIZET, Y., MÜNTENER, O., ULMER, P. & WEBSTER, J.D. (2005): A composition-independent quantitative determination of the water content in silicate glasses and silicate melt inclusions by confocal Raman spectroscopy. *Contrib. Min. Petrol.* **150**(6), 631–642.

MELT INCLUSIONS IN PLUTONIC ROCKS

Mineralogical Association of Canada
Short Course Series Volume 36

Edited by

James D. Webster
Department of Earth and Planetary Sciences,
American Museum of Natural History,
Central Park West at 79th Street,
New York, NY 10024-5192, USA

Short Course delivered in association with the annual meeting of the Geological Association of Canada and the Mineralogical Association of Canada, Montreal, Quebec, 13–14 May, 2006.